



CHALMERS
UNIVERSITY OF TECHNOLOGY

The effect of PLGA nanoparticles on the adipogenic commitment of human mesenchymal stem cells

Master's thesis in Biotechnology

SIMON MYRBÄCK

MASTER'S THESIS 2017

**The effect of PLGA nanoparticles on the
adipogenic commitment of human mesenchymal
stem cells**

SIMON MYRBÄCK



CHALMERS
UNIVERSITY OF TECHNOLOGY



Department of Physics
Division of Biological Physics
CHALMERS UNIVERSITY OF TECHNOLOGY
Gothenburg, Sweden 2017

The effect of PLGA nanoparticles on the adipogenic commitment of human mesenchymal stem cells
SIMON MYRBÄCK

© SIMON MYRBÄCK, 2017.

Supervisor: Qing Ling Feng, School of Materials at Tsinghua University
Examiner: Julie Gold, Department of Physics, Chalmers University of Technology

Master's Thesis 2017
Department of Physics
Division of Biological Physics
Chalmers University of Technology
SE-412 96 Gothenburg
Telephone +46 31 772 1000

Typeset in L^AT_EX
Printed by Chalmers Reposevice
Gothenburg, Sweden 2017

The effect of PLGA nanoparticles on the adipogenic commitment of human mesenchymal stem cells

SIMON MYRBÄCK

Department of Biological Physics
Chalmers University of Technology

Abstract

Poly (Lactic-*co*-Glycolic) Acid (PLGA) is a widely used polymer that is approved to use in biomedical applications. Current studies try to incorporate the versatile nature of the polymer in the biomedical field as drug delivery vectors. This master's thesis aimed at producing PLGA nanoparticles and determine if they have any effect on the adipogenesis from Human Mesenchymal Stem Cells (hMSCs). Nanoparticles were synthesised by an emulsification-solvent evaporation method which resulted in monodispersed particles with a hydrodynamic radius of ~ 350 nm. The synthesised particles had a ζ potential close to zero indicating of an unstable dispersion. After γ irradiation, the particles fragmented and aggregated forming both nano and micro sized agglomerates. When exposing the hMSCs to a range of concentrations of the sterilised PLGA nanoparticles, it was shown to have a short term toxicity on hMSCs, but no effect on adipogenesis was detected.

Keywords: PLGA, nanoparticles, hMSC, adipocyte, adipoigenic differentiation, solvent evaporation method.

Acknowledgements

I would like to express my most sincere gratitude to professor Qing Ling Feng, who made my trip to China and this thesis possible. Through her, I got to experience the prestigious Tshinghua University and to learn about the ancient history as well as daily life of China and Chinese people. Furthermore, I would also like to thank the group of excellent scientists in her research group, namely Wei He, Xujie Liu, Qianli Huang, Ranran Zhang, Yuanyuan Li, Xing Yang and Li Zheng, for always helping me when I was lost in the lab. I will always be thankful to my mentor, Tarek Elkhooly, who was the expert as well as moral support, with the occasional and much appreciated Arabian coffee, through the entire thesis. In addition, I would like to thank Julie Gold at Chalmers University for accepting to be my examiner, but mostly for her support and inputs while I wrote this thesis. Lastly, I would like to express my appreciation to Lukas Dahlgren, my brother-in-arms through this adventure.

Thanks, xiéxie, shukran and tack!

Simon Myrbäck, Gothenburg, June 2017

Contents

List of Figures	xi
Abbreviations	xiii
1 Introduction	1
2 Theory	3
2.1 Poly (Lactic- <i>co</i> -Glycolic) Acid	3
2.1.1 Synthesis of PLGA nanoparticles	4
2.1.2 Storage and utilisation	6
2.1.3 Characterisation techniques	7
2.2 Adipocytes	9
2.2.1 Cellular uptake	11
2.2.2 Cytotoxicity and differentiation	11
3 Methods	13
3.1 Particles	13
3.1.1 Synthesis	13
3.1.2 Characterisation	14
3.2 Cell culture evaluation	14
3.2.1 Adipogenesis	15
3.3 Statistics	17
4 Results	19
4.1 Particle characterisation	19
4.2 Cell culture evaluation	22
5 Discussion	27
5.1 Particle characterisation	27
5.2 Cell culture evaluation	28
5.3 Future	30
6 Conclusion	31
A Appendices	I
A.1 Appendix I	I
A.2 Appendix II	II

List of Figures

2.1	Chemical structure of the monomers constituting PLGA	3
2.2	Chemical structure of PLGA	4
2.3	The emulsification-solvent evaporation method	5
3.1	Flowchart of cell culture evaluation	16
3.2	Staining with Oil Red O from previous studies.	17
4.1	DLS measurement in deionized water	19
4.2	DLS measurement in growth medium.	20
4.3	DLS measurement in complete growth medium	20
4.4	DLS measurement of γ irradiated particles in complete growth medium.	21
4.5	Measured ζ potential of PLGA particles.	21
4.6	SEM pictures of PLGA particles.	22
4.7	The effect of gold vs platinum sputtering on PLGA nanoparticles, 25 kx magnification	22
4.8	SEM images of PLGA nanoparticles encapsulated in trehalose.	23
4.9	CCK8 viability test of hMSC's.	23
4.10	Confocal images of expressed adiponectin.	24
4.11	Confocal images of PPAR γ	25
4.12	Quantitative study of secreted adiponectin.	25
4.13	Oil Red O staining of the fat droplets	26

Abbreviations

ATP	Adenosin Triphosphate
BMP4	Bone Morphogenic Protein 4
C/EBP α	CCAAT-Enhancer-Binding Proteins- α
C/EBP β	CCAAT-Enhancer-Binding Proteins- β
cAMP	Cyclic Adenosine Monophosphate
DAPI	4',6-diamidino-2-phenylindole
DLS	Dynamic Light Scattering
FBS	Fetal Bovine Serum
FDA	U.S. Food and Drug Administration
HAELISA	Human Adiponectin Enzyme-Linked Immunosorbent Assay
hMSC	Human Mesenchymal Stem Cell
IGF1	Insulin-like Growth Factor 1
IMX	3-isobutyl-methylxanthine
LG-DMEM	Low Glucose - Dulbecco's Modified Eagle Medium
PBS	Phosphate Buffer Solution
PdI	Poly-dispersive Index
PLGA	Poly (Lactic- <i>co</i> -Glycolic) Acid
PPAR γ	Peroxisome Proliferator-Activated Receptors- γ
PVA	Poly Vinyl Alcohol
ROS	Reactive Oxygen Species
SEM	Scanning Electron Microscope
UCP1	Un-Coupling Protein 1

1

Introduction

One of the current biggest health problems in today's society is obesity, with over 37 % of the world's adult population being overweight (BMI >25 kg/m²) and over 20 % of Europe's adult population being obese (BMI >30 kg/m²) (Ng et al. 2014, WHO 2013). Obesity is a chronic disease that increases the risk for a multitude of health problems; diabetes, high blood pressure, cardiovascular disease, stroke, arthritis and cancer, impairing physical and mental health as well as increasing the risk of premature mortality (Twells 2015). Due to the large part of the population being affected, the economic impact of obesity is important but difficult to determine. The cost is divided into direct medical cost, which is the spending to diagnose and treatment of the serious health conditions related to obesity, and indirect cost, which is due to absenteeism, decreased productivity, disability, health insurance costs and premature mortality. The overall economic impact of obesity is significant, predicted to cost over \$215 billion dollar in the US alone in 2010 (Hammond & Levine 2010), and increases as the epidemic disease continues to spread.

To combat the threat of increasing obesity, the World Health Organization (WHO) is advocating for a broad spectrum of treatments, targeting both private persons and companies view and actions on health issues (Quintiliani 2007). The first step towards a healthy lifestyle is to limit calorie intake and exercising according to recommendations, but a majority of patients (~ 70 %) regain some or all of the weight lost over time (Anderson et al. 2001). When this is not sufficient and a person is in need of medical help the options are limited. Bariatric surgeries are effective at helping obese patients lose and maintaining weight, although at high risks of complications (O'Brien et al. 2013, Buchwald et al. 2004, Pories 2008). Scientists are currently looking at weight reducing drugs, which increase the weight loss when combined with other weight reduction measurements (Yanovski & Yanovski 2014). This will further help those afflicted by the chronic disease, decreasing health risks and medical costs to a large portion of the population.

There are a few crucial points when administering these drugs; solubility, survivability and release profile. By encapsulating the drug in a polymer and aggregating it into a tablet, the crucial points can be satisfied. However, if the patient receives treatment orally, the drug effects the entire body. This might in turn give rise to other limitations. These limitations can be controlled by administering the drug intravenously instead. If the latter technique is used, the size of the tablet has to be small enough as to not get stuck in the blood stream. To administer the weight reducing drugs, PLGA polymers can be used as encapsulation agents. The loaded

particles can then be surface modified to allow for fat tissue-specific targeting of the obesity drug, which limits any systemic effects (Fahmy et al. 2005). When the particles are in close proximity to the cells, they might get endocytosed through either phagocytosis or pinocytosis. Phagocytosis is limited to a few cell types, such as macrophages and neutrophils which sole purpose is to "eat and digest" foreign material, while pinocytosis can be performed by all cells but is limited to small sizes of particles (Tabata & Ikada 1988, Kohane 2007). If the targeted cell type is adipocytes, the particles need to be small enough for the fat cells to pinocyte them to allow intracellular release (Kohane 2007). However, the exact biological fate of the PLGA nanoparticles are not yet known after entering the cell and more research is needed (Panyam & Labhasetwar 2003).

Once the particles are inside the cells, the drug is released and has a well documented effect on the organism. However, current research has found that the PLGA nanoparticles themselves affects the hMSCs in several ways. For example, they increase both Reactive Oxygen Species (ROS) generation and expression of inflammatory cytokines (Kanda et al. 2011). The first increases adipogenesis through activation of Peroxisome Proliferator-Activated Receptors- γ (PPAR γ) and the second might have cytotoxic effects on the cells. The variances between different cell lines indicates that more research is needed to fully understand and eventually predict how PLGA nanoparticles affects the entire human body (Fröhlich et al. 2012).

The aim of this master thesis is to synthesise unloaded PLGA nanoparticles through a single emulsification-solvent evaporation method and then determine if they have any effects on the adipogenic differentiation of hMSCs. The thesis will be limited to one size of nanoparticles produced by one method as described below. The cell tests will not have more than three repeats, all done on the same well plate. All particle exposures will be done at six different concentrations of particles except confocal imaging which will have three (including control).

2

Theory

2.1 Poly (Lactic-*co*-Glycolic) Acid

PLGA is commonly used as drug vehicle due to its biocompatible and biodegradable nature in several different applications in the human body. The polymer consists of two monomers, glycolic and lactic acid, which the body can degrade through the metabolism. The two different monomers have a slight different structure, the glycolic acid (Figure 2.1a) lacks a methyl side group when compared to lactic acid (Figure 2.1b). This difference makes the polymer of glycolic acid a more hydrophilic polymer with higher crystallinity and faster degradation time when compared to the polymer of lactic acid (Gentile et al. 2014).

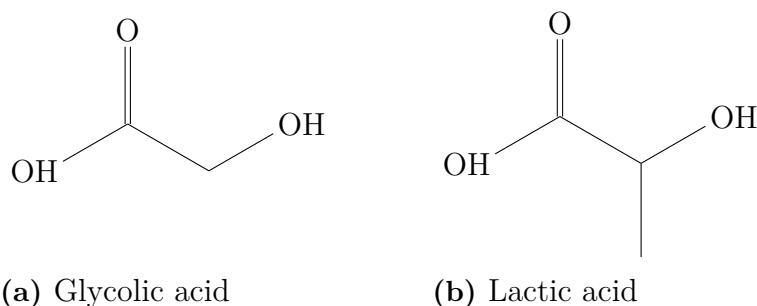


Figure 2.1: Chemical structure of the monomers constituting PLGA

Due to the different physicochemical properties of the monomers, PLGA (Figure 2.2) can be tailored to a large extent depending on the intended use. For instance, by varying the ratio of the monomers a wide range of degradation rates, mechanical strength, solubility and viscosity can be achieved (Wang et al. 2006). However, the same ratio of the monomers can give rise to different physicochemical properties through the tacticity of the constituents, an atactic polymer degrades faster than an iso- or syndiotactic polymer. The degree of tacticity is determined during the polymerisation process; a ring-opening process can achieve an atactic or syndiotactic product depending on the choice of catalyst (Dechy-Cabaret et al. 2004, Li et al. 2011).

The choice of catalyst affects the product and efficiency of the process but it might be at a cost of post-polymerisation procedures. A metal catalyst is most commonly used due to the high efficiency, but they are generally not approved in the human

body. Stannous octoate (SnOct_2) is an exception, being approved as a food additive which simplifies any larger production of PLGA for the biomedical field (Kricheldorf et al. 1992, Kowalski et al. 2000). Furthermore, the chiral nature of lactic acid also affects the PLGAs chemical and physical properties. When comparing the outcome of two esterification polymerisation processes, one with L-lactic acid and one with a racemic mix, the molecular weight varied (Stayshich & Meyer 2008). This indicates different physicochemical properties coupled to the chirality of the polymer.

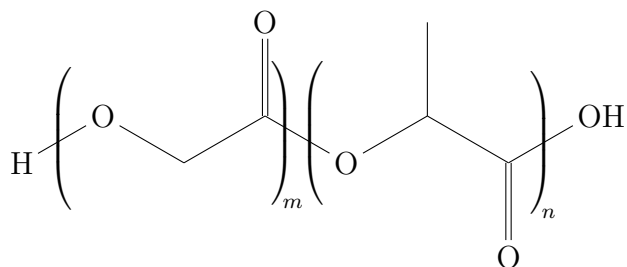


Figure 2.2: Chemical structure of PLGA

2.1.1 Synthesis of PLGA nanoparticles

There are several different techniques to synthesise PLGA nanoparticles, emulsification solvent evaporation method being one of the common methods in the biomedical applications. The method utilises micelles to form nanoparticles by first solving the polymer in an organic solvent and then adding it to an aqueous solution containing an emulsifier. The solution is then turned into an emulsion by exposing it to shear stress, e.g. by an ultrasonicator or high speed stirring. The applied forces breaks the organic phase into nanosized spheres and the emulsifier decreases the surface tension to allow a stable emulsion. The organic solvent is then removed by evaporation while stirring, and as it is removed the polymer precipitates forming particles. The method can be altered to include a second water phase inside the organic phase. This is done by first adding a small amount of water into the organic phase with an emulsifier and then applying shear stress. This first emulsion is then used as the organic phase previously described.

In the organic solution, the choice of organic solvent is important for the final size of the particles. A partially water-soluble substance is preferred due to the decreased surface tension between the phases (e.g. ethyl acetate or propylene carbonate), but viscosity is also important for the efficacy of shear stress as well as the evaporation properties. Polymer concentration has no direct size-dependency, but it is coupled to the amount of needed surfactant later on (Astete & Sabliov 2006). As the organic phase is added into the water phase, the phase ratio is correlated to the particle size. The choice of surfactant is determined both by the organic solvents properties but also by the toxicity when the targeted application is in the biomedical area. The chemical properties of the surfactant determines the stability of the micelles by decreasing the surface tension, but it can also act as a repellent between the micelles

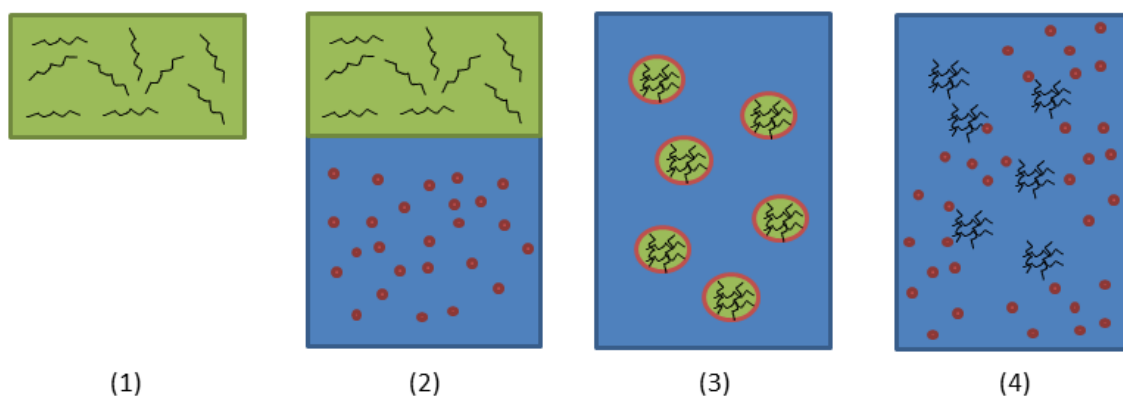


Figure 2.3: A graphic interpretation of the emulsification solvent evaporation method. The polymer is solved in an organic solvent (1) and then added into a larger volume of aqueous solution with emulsifier, red (2). The solution is then exposed to shear stress and the organic phase forms micelles with the emulsifier on the surface (3). The organic solvent is then evaporated and nanoparticles are formed (4).

due to electrostatic properties if the surfactants are charged (Song et al. 2006). The total amount of shear stress that the two phases are exposed to are critical to size. To form a stable emulsion of nanosized micelles, the agitation needs to be strong enough to reduce the droplet size while also being long enough to make sure the equilibrium to be stable (Astete & Sabliov 2006). PLGA has a low glass transition temperature and ultrasonicators can increase the temperature through the addition of energy. Therefore, it is crucial to keep the solution on ice to keep it below this critical level. After the emulsion is formed, the evaporation of organic solvent is crucial. Coalescence can occur as long as there is organic solvent present, and by decreasing the time of evaporation the risk of increased size over time is lowered. To be able to use the particles in any biological tests, removing the emulsifier is crucial. Some emulsifiers are lethal for the cells as they interact with the cellular membrane, while others only affect cellular uptake (Sahoo et al. 2002).

Other methods to synthesise nanoparticles are nanoprecipitation and salting out. During both these methods, the polymer is dissolved in a water-miscible organic solvent. The nanoprecipitation then forms particles by pouring the organic phase into the water phase in a controlled manner. The nanoparticles are formed instantaneously due to the rapid solvent diffusion from the polymers into the bulk water phase and later removed by evaporation under reduced pressure. The salt out method requires strong mechanical stress to form the micelles, at the presence of high concentration of salt ions in the water phase. The salt inhibits any diffusion of organic phase until large amounts of pure water is added quickly. This method requires a purification step to remove the salt (Astete & Sabliov 2006).

2.1.2 Storage and utilisation

After the production and purification of the nanoparticles, the next critical obstacle is the storage. The PLGA nanoparticles unstable nature in medium, due to aggregation of particles and hydrolysis of polymer, makes the step crucial for any practical utilisation of the particle-based system. The most common method to increase the shelf time is lyophilisation, freeze-drying. The suspended particles are first frozen in a tube in a low-temperature freezer until completely frozen. The lid is removed and the tube is then moved into the lyophilizer at low temperature and low pressure. This keeps the sample frozen while the close-to-vacuum allows for sublimation and desorption of the water. The low pressure might also remove some particles and a thin barrier might be added to allow water diffusion but keep the particles in the tube. The process puts the particles to different stresses as well as an increased risk of aggregation and irreversible fusion. This is limited by adding a cryoprotectant to protect the nanoparticles from freezing and desiccation stresses (Abdelwahed et al. 2006). If a cryoprotectant is used, the temperature of storage, and of the initial freezing, needs to be lower than the glass transition temperature of the protectant to prevent product collapse (Holzer et al. 2009).

The degradation of PLGA particles is biphasic. The first step is heterogeneous autocatalysis that is dependent on the accumulation of degradation products (oligo- and monomers). The concentrated acids give rise to a decrease in pH inside the particles which catalyses the de-esterification process (Li & Vert 2002). This requires the particle to be larger than 300 nm and have a limited porosity, smaller or high porosity particles allow for the diffusion of the degradation products (Dunne et al. 2000). As the degradation progresses, the mobility of each polymer increases which allows for crystallisation and a decrease in degradation rate. Over time, the bulk degradation is getting equal to surface degradation and the overall deterioration of the particle is getting more homogenous. This characterises the second phase during which the mass loss is not dependent on the size of the particle (Spentehauer et al. 1989). Higher porosity allows for more water to diffuse into the particle which increases the overall deterioration of the particle. Furthermore, hydrophilicity allows for more water to diffuse into the particle which allows for a faster hydrolysis. Given the complex nature of the degradation profile of the polymer, it is hard to formulate particles with a narrow degradation rate to be used in the pharmaceutical field (Anderson & Shive 2012).

If the intended field of application is biomedical, the particles also has to undergo sterilisation before usage. There are several sterilisation procedures, but water sensitivity of the PLGA particles makes γ irradiation, ethylene oxide and filtering possible. The γ irradiation procedure applies the damaging affect on biological tissues from γ rays to lower the amount of biological active organisms. However, the rays also introduce instability, deterioration, cross-linking breakage of polymer chains and heat (Dillen et al. 2004, Lü et al. 2009). These factors combined can damage the polymer to the point where it fragments or melts together. Later studies allowed the same group of scientists to save the particles by adding a cryoprotectant and reported an increased work required to resuspend the sterilised particles

(Bozdog et al. 2005). The protected particles would be unscathed, keeping both hydrodynamic radius and ζ potential during the sterilisation process. However, both previous studies performed the Dynamic Light Scattering (DLS) measurements in serum free solutions, removing any effects proteins might have on the results.

Exposing the PLGA nanoparticles to ethylene oxide would be another sterilisation technique. This method relies on the high reactivity of the ethylene oxide as it diffuses fast. This allows for an easy access to different cellular compartments, which the ethylene oxide then inactivates through alkylation. The addition of alkyl groups to macromolecules in the cell, such as proteins, DNA and RNA prevents normal cellular metabolism and reproduction (Mendes et al. 2007). Previous work with ethylene oxide sterilisation has shown to not effect the molecular weight, surface composition, mechanical properties, or *in vitro* degradation rate of poly lactic acid (Hooper et al. 1997). The filtering technique relies on the size of the contamination and a membrane with pores of a well defined size. The common size of the pores are around $0.2 \mu\text{m}$, which separates bacteria and cells from the solution but viruses and phages as well as secreted proteins can pass through. This procedure is easy to use in large scales, but might require a high pressure to be efficient.

2.1.3 Characterisation techniques

This section will describe the Scanning Electron Microscope (SEM), DLS and ζ potential measurement techniques used to evaluate the PLGA nanoparticles in more details.

2.1.3.1 Scanning Electron Microscope

The SEM technique works by bombarding the sample with a thin beam of high energy electrons and then measure the emitted electrons. The beam is generated and accelerated in the electron gun, where the electrons are excited through thermionic emission. This is done by leading a high current through a thin specimen of e.g. tungsten, which creates thermal energy. When this energy is increased above the work function of the material, an electron is emitted. The electron beam is then demagnified by passing through two condenser lenses, forming the primary beam which is then passed through the objective lens. The objective lens focuses the lens to certain places of the specimen, and the SEM utilises this in a raster-fashion to scan the entire sample. As the electron beam hits the sample, new electrons as well as X-rays and visible light are emitted and these are in turn measured. The electrons can be emitted by two different mechanisms, giving rise to electrons with different energy. Secondary electrons are formed as ionisation products, with less energy, due to the primary beam. Back scattering electrons are reflected electrons from the primary beam and has higher energy, but maximum equal the energy of the primary beam. The Auger effect also gives rise to sample characteristic electrons depending on the material of the sample. The photons emitted as X-rays can be used to identify the material of the sample and the emitted light can be used to

image semi-conductive defects (Khursheed 2011).

One of the limitations of SEM is that the material needs to be conductive and grounded in order for it to not accumulate electrostatic charge. PLGA nanoparticles are not conductive and need to be prepared with a thin layer of metal before being imaged in the SEM. This can be done by sputtering, during which a metal of choice (e.g. gold or platinum) is being bombarded with high energy atomic particles. The atomic particles increase the thermal energy in the surface until individual atoms are removed via collision processes. The free atoms then form a thin layer on the probe as they cool down (Stuart 1983). Sputtering of gold and platinum has previously been done on PLGA nanoparticles (Cartiera et al. 2009, Win & Feng 2005).

2.1.3.2 Dynamic Light Scattering

The DLS measurement relies on laser technique to measure how fast the particles move in the sample. This movement is then used in the Stokes-Einstein equation to calculate the hydrodynamic radius of the particles. The monochromatic light is first shot through a polariser and then through the sample. The scattered light passes through a second polariser before being collected and imaged on a speckle pattern. This is repeated within a short time interval and the different speckle patterns are then compared to determine how far the particles have moved. This fluctuation is due to Brownian motions, which is correlated to the size of the particle, the properties of the solution and temperature. The equation assumes all particles to be monodisperse spheres, imposing limitations if this is not true. The calculated hydrodynamic radius is also dependent on any surface active substance, such as ions or proteins (Berne & Pecora 2000). If ions are present, they adsorb onto the surface and forms layers around the particle, called double layers. These layers interfere with the movement as the double layers interact with the slipping plane layer, which consists of free moving ions, and decreases the speed which makes the particles seem bigger than in pure water. The proteins adsorb onto the surface due to several driving forces, such as intermolecular forces, surface energy, hydrophobicity and ionic or electrostatic interactions. The adsorbed proteins makes the particle more bulky, limiting movements, but also increases the surface area which allows for more ions to adsorb if they are present.

2.1.3.3 ζ potential

The measurement of the ζ potential works by the same principal as DLS measurement, with the addition of an applied voltage. This applied voltage also applies a force on the dispersed particles, and the laser technique is then used to evaluate the velocity this force puts the particles in. This mobility is then converted to ζ potential by taking the dispersant viscosity and dielectric permittivity into account as well as using the theories of Smoluchowski (1903). This theory simplifies the model by neglecting the contribution of surface conductivity by assuming that the

double layer is much smaller than the particle radius. This is valid for particles that are larger than $1 \mu\text{m}$ in aqueous milieu. However, if the particles are in the nano scale, the ionic strength of pure water is too high for this model and a small amount of ions is added to decrease it (Malvern.com 2017).

2.2 Adipocytes

For decades, scientists considered adipose tissue to be an inert mass which stored energy, isolated the body and mechanically supported important structures. The awareness of adipocytes role as essential regulators of whole-body energy homeostasis started with the identification of leptin in 1994 (Zhang et al.). When Taylor & Jones (1979) managed to differentiate hMSC into adipocytes, cartilage and muscle cells, scientists had received a base to systematically study the properties of the adipocytes. The enigma started to unravel.

Today, researchers know that there are two types adipocytes which can be found in a large variation of tissues and niches. The white adipocytes role is to keep the body's energy balance. This is mainly done by the storage of triglycerides and release of fatty acids when energy expenditure is high and low respectively. The triglycerides are stored in large fat droplets. However, the white adipose tissue also has a function as an endocrine organ (Vázquez-Vela et al. 2008). The second type of fat cells is the brown adipocytes. These cells have a numerous amount of small lipid droplets, a higher concentration of mitochondria and utilise the Un-Coupling Protein 1 (UCP1). UCP1 uncouples the Adenosin Triphosphate (ATP) synthesis and allows futile cycles of metabolism to run. This gives the brown adipocytes the ability to catabolise energetic molecules at a high rate without accumulating ATP and only generating heat (Seale et al. 2011). White adipose tissue can be found mainly in two different tissues, visceral and subcutaneous fat. Brown adipose tissue is most prevalent at infancy, and only small amounts persists until adulthood spread out in small depots in the thorax. Furthermore, beige adipocytes exists which originates from white adipocytes that transdifferentiate to expressing UCP1 but fail to express myorelated markers (Wu et al. 2012).

The differentiation of adipocytes from hMSCs occurs in two steps, determination and terminal maturation. During the determination the stem cells lose its pluripotency, stop dividing and form a preadipocyte. The preadipocyte is not morphologically different from its precursor, but committed towards adipogenesis (Rosen & MacDougald 2006). The genetic mechanism that controls the initiation of the determination is known to a large extent. Bone Morphogenic Protein 4 (BMP4) is thought to have an essential role, but Wnt signaling, cell density and cell shape also play a role in the complex lineage commitment that still elude the scientists (Otto & Lane 2005, Bowers & Lane 2007). However, if the hMSC is exposed to an activator of PPAR γ expression, the cell also enters the adipogenesis (Otto & Lane 2005). Next follows the terminal maturation, during which the preadipocyte activates genes and markers and undergoes morphological change towards a mature adipocyte. The process is activated by Insulin-like Growth Factor 1 (IGF1), glu-

cocorticoid agonist and an agent that increases Cyclic Adenosine Monophosphate (cAMP). The process is characterized by a rapid and transient increase in CCAAT-Enhancer-Binding Proteins- β (C/EBP β). The mature adipocyte expresses certain phenotype specific markers and specifically PPAR γ is often targeted by immunohistochemistry (Otto & Lane 2005). The adipocyte is able to transport large amounts of glucose in response to insulin, to synthesise fatty acids and to store, and hydrolyse in time of energy deprivation, triacylglycerols (Fève 2005). By exposing the cells to insulin throughout the differentiation process, the amount of synthesised and accumulated triglycerides increases (Green & Kehinde 1975). The stored triacylglycerols can be screened for by using fat-soluble dyes.

One of the niches where adipocytes are crucial for the tissue is in bones. Adipocytes and osteoblasts share the same progenitor and are differentiated in a reciprocal manner, for example PPAR γ activates adipogenesis while it decreases osteogenesis (Nuttall et al. 2014). Even though this is a simplified example, it highlights how complex the body's regulation of organs and tissue is.

Adipose tissue consists of connective tissue matrix, nerve tissue, stromovascular and immune cells. Together they function as an integrated unit. The tissue is an essential and highly active metabolic and endocrine organ. It responds to afferent signals from traditional hormone systems and the central nervous system as well as it expresses and secretes factors with important endocrine functions (Kern et al. 2003). One of these factors is leptin, the starter of adipose tissue research. Leptin is important in energy balance and is expressed and secreted in proportion to adipose tissue mass as well as nutritional status (Fain et al. 2004, Wajchenberg 2000). It is further increased by insulin, CCAAT-Enhancer-Binding Proteins- α (C/EBP α) and decreased by free fatty acids and PPAR γ , to describe some of the adipocyte specific enzymes influence on the adipogenic differentiation (Margetic et al. 2002). The effects of leptin on energy homeostasis are mediated through several different systems. Hypothalamic pathways particularly focus on energy intake and expenditure and direct action on peripheral tissues including muscle and pancreatic β -cells (Bjorbæk & Kahn 2004). Leptin has further effects, including neuroendocrine function, regulation of immune function, hematopoiesis, angiogenesis, and bone development (Bjorbæk & Kahn 2004, Lord et al. 1998).

Another important protein that adipose tissue expresses and secretes is adiponectin. The phenotypic marker circulates the blood stream at high levels and is expressed at higher levels in subcutaneous adipose tissue, rather than visceral adipose tissue (Chandran et al. 2003, Fain et al. 2004). Researchers have found an inverse association between adiponectin and both insulin resistance and inflammatory states, which has been established to be both strong and consistent. When administered to obesity or lipodystrophy caused insulin resistant, the metabolic parameters improves. Adiponectin levels increase when insulin sensitivity improves, which occurs after weight reduction of obese individuals (Diez & Iglesias 2003, Chandran et al. 2003, Kinlaw & Marsh 2004). The exact mechanism of expression of adiponectin is not currently known, but the secretion is induced during early adipogenesis and

then down-regulated in the terminal step (Qiang et al. 2007).

2.2.1 Cellular uptake

Endocytosis of particles are divided into three pathways; receptor-mediated endocytosis, phagocytosis and pinocytosis. Different cell types use the systems to different extent; macrophage's role is to phagocytose and degrade objects and compounds while smooth muscle cells mostly uses receptor-mediated endocytosis and pinocytosis (Panyam & Labhasetwar 2003). The particles stay in the cell as long as the concentration gradient exists and when the particles are washed away, the intracellular concentrations rapidly falls. The particles are efficiently taken up through an endocytosis mechanism in an inverse size dependent way, and escape into the cell cytosol from the very start. Particle uptake has been shown to be temperature and native cell function dependent (Cartiera et al. 2009). This indicates that treatments are efficient as soon as administered and smaller particles are more efficient drug vectors, but that the extracellular concentration of particles are crucial for longer term exposure (Panyam & Labhasetwar 2003). The lysosomal escape is needed for the drugs to be released in a non-destructive environment (release inside lysosomes does naught as treatment). The body removes larger particles in the vascular system through the spleen in a size dependent way but studies has shown that drugs stay in the tissue for up to 14 days. This would make treatments with nanoparticles that were administered locally in the close tissue efficient (Müller et al. 2003, Fishbein et al. 2001). Another property of the PLGA nanoparticles that affect cellular uptake is the surface charge. It has been theorised that the negatively charged cellular membrane and intracellular environment allows for a quick endocytosis of positively charged particles (Platel et al. 2016). A neutral surface charge would result in a minimal cell to particle interaction due to the decreased amount of adsorbed proteins while a negative charge would be repelled by the cellular membrane, both leading to a lower cellular uptake then positively charged particles (Verma & Stellacci 2010). Furthermore, the tissue distribution of the microspheres might be guessed depending on which proteins adsorb to the surface of the particles, indicating possible site targeting (Müller et al. 2003). However, these findings are collected from a variety of particle materials and might not be completely applicable to PLGA.

2.2.2 Cytotoxicity and differentiation

PLGA is a biomaterial approved by the U.S. Food and Drug Administration (FDA) in several biomedical applications, such as drug delivery vehicle and implants. To get the FDA approval the material had to be thoroughly tested both as scaffolds and as particles, depending on the type of usage in each application. Studies have found PLGA to be sufficiently biocompatible, although with some adverse effect. The concern rises from several sources. The acidic degradation products that PLGA give rise to might have a cytotoxic effect in tissues with large amounts of the polymer, such as close to an implant. This is of major concern in the orthopaedic applications, but

less in nanotechnology unless the intracellular concentration is high (Gunatillake & Adhikari 2003). Xiong et al. (2013) has found that PLGA nanoparticles exhibit a size-dependent cytotoxicity. The mode of action is suggested to be that smaller particles have a higher surface area to volume ratio and that different types of proteins adsorb to the surface. These proteins might then get damaged, thus triggering a negative cascade inside the cells. The cellular damage that these give rise to include an increased generation of ROS, mitochondrial depolarisation, plasma membrane leakage, increased intracellular calcium concentration and inflammation response.

Further on, the increased generation of ROS has shown to be linked to an increase in adipogenesis (Kanda et al. 2011). Scientists theorise that the ROS is required for adipocyte generation through the activation of PPAR γ , which is the master regulator of adipogenesis (Tormos et al. 2011). The surface topology, charge and hydrophobicity are other factors that influence the generation of ROS as well as cytotoxicity (Fröhlich 2012). However, most of the used PLGA nanoparticles in research are coated with either another polymer (such as chitosan) or other molecules (such as bovine serum albumin). By adding this layer, the inflammatory response that was previously found had been negated and any effect on differentiation should thereby decrease (Jiang et al. 2015, Mura et al. 2011). This might be due to the changed surface composition, which changes the amount and types of proteins that adsorb to it as the cell takes up the particle. Other studies have found that a positive surface charge is allowing the particles to react with the negatively charged DNA, lowering cell viability (Singh et al. 2009, Platel et al. 2016). Neither a neutral or a negative surface has been shown to have any effect on the cytotoxicity (Platel et al. 2016). However, a large variance between different cell lines was found in Fröhlich et al. (2012) study, demonstrating the importance of evaluating all cell types.

To evaluate the synthesised particles, a Cell Counting Kit-8 is performed. The test is done by exposing all cells to WST-8, a slight yellow dye, which is reduced by dehydrogenase activities. This enzyme is only present when living cells synthesise it. The reduced orange dye, WST-8 Formazan, is then measured by a spectrophotometer and the absorbance is directly correlated through the enzyme activity to the living cell concentration (Dojindo 2016).

3

Methods

This master's thesis is divided into two main steps; PLGA nanoparticle synthesis and hMSCs evaluation. In brief, PLGA nanoparticles were synthesised through an emulsification-solvent evaporation synthesis method and then characterised to determine physical and chemical properties. The hMSCs were then subjected to these particles while being differentiated toward adipocytes, and different adipogenic markers were investigated to determine the adipogenesis.

3.1 Particles

Below, the PLGA nanoparticle synthesis is described in more details. The nanoparticles were synthesised through an emulsification-solvent evaporation protocol. The characterisation was then performed through SEM imaging, measuring hydrodynamic radius with DLS as well as determining the ζ potential.

3.1.1 Synthesis

An oil/water emulsification solvent evaporation method was used to synthesise the particles. 200 mg 50:50 PLGA polymer ($M_w = 70-88$ kDa) was dissolved in 2 ml ethyl acetate by stirring to get a 10 % solution, called organic phase. 40 mg Poly Vinyl Alcohol (PVA) ($M_w = 30-70$ kDa, 87-90 degree of hydrolysis) was dissolved in 4 ml deionised water to get a 1 % solution, called external phase. The organic phase was then added into the external phase while vortexing. The primary emulsion was moved into an ice bath and put in the ultrasonicator. Subsequently, the sample was sonicated with 50 W for 3x10 seconds with 10 seconds rest in between each run. The secondary emulsion was poured into an evaporation phase (100 ml 0.1 % PVA in deionised water) and left over night, while stirring, to evaporate the organic solvent. To wash away the PVA, four washing steps were performed. Each washing step was performed by centrifuging the sample in 12 000 RPM (7200 G) for 10 mins, 20 °C, discarding the supernatant and then followed by addition of deionised water and vortexing as well as brief sonicating to resuspend the PLGA particles. The last resuspension was performed in 4 ml deionised water and a small aliquot (5 %) was removed for SEM testing. Trehalose was added as a cryoprotectant, in 1:2 weight ratio to trehalose:PLGA. The suspension was moved into a preweight vial and then put into a -80 °C freezer until completely frozen. Once frozen, the lid was replaced

with lab tissue, to allow sublimation while retaining the particles. The container was then transferred into the lyophiliser where the cryoprotected particles were freeze dried in -42°C , 9.8 Pa until completely dry. Afterwards, the vial with particles and trehalose was weighed again and the yield was calculated by removing the known weight of the added cryoprotectant. The particles were later sterilised with 20kGy γ irradiation and stored at -80°C .

3.1.2 Characterisation

To qualitatively determine the size and shape of the particles, SEM was used to get qualitative pictures of size, size distribution and shape. In brief, dried particles were spread on an electrically conducting adhesive, blowing slightly to remove free particles. The sample holder was then given to technicians who sputtered it with gold, 8 mA for 180 s (SBS-12, KYKY Technology Development LTD., China), or platina, 100 mA 300 s (Gatan681, USA), and then inserted into the SEM using a voltage of 5 kV.

To quantitatively determine the size, a DLS measurement was performed. Briefly, the PLGA particles were suspended in deionized water, Low Glucose - Dulbecco's Modified Eagle Medium (LG-DMEM) or LG-DMEM with Fetal Bovine Serum (FBS) until slight turbidity. 10 mmol KCl was added as electrolyte. The test was performed at 25°C and three repeats were performed on each suspension. The ζ potential of the particles was measured to determine the long term stability and risk of aggregation. Particles were suspended in deionized water until slight turbidity and transferred into a vial before measuring the ζ potential at 25°C .

3.2 Cell culture evaluation

hMSCs of 4th passage (Cyagen Biosciences Inc, China) were cultured in basal medium containing 10 % FBS, 1 % penicillin and streptomycin at standard culture conditions (5 % CO_2 , 37°C), medium was changed every second day. Passaging was performed when the confluency reached 80-90 % by trypsinating the cells. The trypsination was performed by adding 2 ml of 0.25 % trypsin and was incubated in standard culture conditions until visual inspection showed that most cells had detached. The cells were then moved into a vial and basal medium supplemented with 10 % FBS to inhibit the enzymatic reaction of trypsin, followed by centrifugation (1000 g, 5 min). The supernatant containing the trypsin was then removed and the cells were resuspended in growth medium (see Table 3.1) followed by plating in two new petri dishes.

To determine the cytotoxicity, a CCK-8 test (Dojindo, Japan) was performed on undifferentiated hMSCs from 10th passage. The cells were trypsinated (0.25 %, \sim 2 min), centrifuged, resuspended in testing medium (see Table 3.1) and transferred into a 24 well plate (Corning, USA). The cells were let to attach for one day and

then exposed to 10, 50, 100, 250 and 500 $\mu\text{g}/\text{ml}$ PLGA nanoparticles in testing medium (see Table 3.1) for one day. Each concentration of exposure was done in three wells on the same plate ($n = 3$). At day 1, 3 and 7 after exposure the cells were washed twice with Phosphate Buffer Solution (PBS) before adding 450 ml medium and 50 ml CCK-8 medium. The cells were then incubated in darkness for 4 hours after which the absorbance (OD) was measured at 450 nm with a microplate reader (EnSpire, PerkinElmer, USA).

Table 3.1: Brief explanation of the different mediums used.

	Growth	Testing	Differentiation	Maintenance
Medium	Basal	LG-DMEM	LG-DMEM	LG-DMEM
FBS	10 %	10 %	10 %	10 %
Penicillin	0.5 %	0.5 %	100 U/ml	100 U/ml
Streptomycin	0.5%	0.5 %	100 ppm	100 ppm
Glutamine	1 %	–	–	–
Insulin	–	–	10 $\mu\text{g}/\text{ml}$	10 $\mu\text{g}/\text{ml}$
Dexamethasone	–	–	1 μM	–
3-isobutyl-methylxanthine (IMX)	–	–	0.5 mM	–
Indometacin	–	–	200 μM	–

3.2.1 Adipogenesis

To induce the adipogenesis, the hMSCs from 7th passage were trypsinated (0.25 %, ~ 2 min), centrifuged, resuspended in testing medium (see Table 3.1) and seeded into a 48 well plate. When the confluency reached 90 % the cells were exposed to PLGA nanoparticles in testing medium (see Table 3.1) for one day. After the particle exposure, the medium was changed to differentiation medium, containing LG-DMEM supplemented with 10 % FBS, 1% penicillin and streptomycin, 10 $\mu\text{g}/\text{ml}$ insulin, 1 μM dexamethasone, 0.5 mM IMX and 200 μM indometacin. After two days, the medium was changed into adipocyte maintenance medium, containing LG-DMEM supplemented with 10 % FBS, 1% penicillin and streptomycin and 10 $\mu\text{g}/\text{ml}$ insulin, and changed every second day. See Table 3.1 for details on the different solutions used.

Confocal imaging of immunostained PLGA and adiponectin, Oil Red O staining and adiponectin secretion was used to determine the effect of PLGA nanoparticles on the adipogenic differentiation. Figure 3.1 describes the work process on the differentiated cells, more detailed methodology follows below in corresponding section.

3.2.1.1 Immunohistochemistry

hMSCs on day 14 of adipogenic induction, exposed to 0, 100 and 500 $\mu\text{g}/\text{ml}$ particles, where incubated with 0.1% Triton X-100 for 15 minutes to permeabilize the

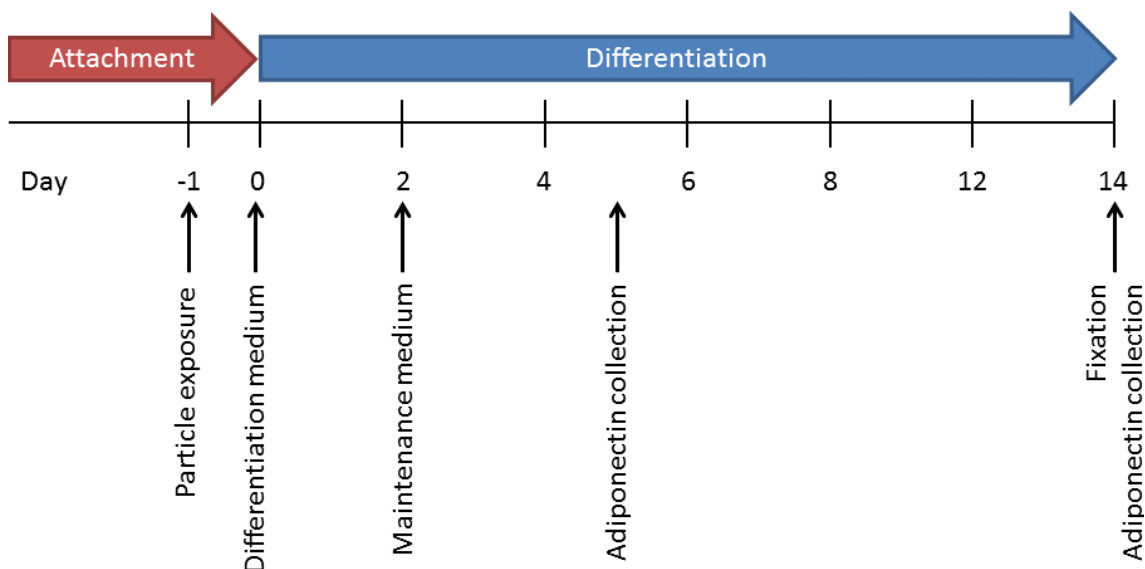


Figure 3.1: A flow chart of the working process on differentiated cells. The exposure was done during 24 hrs and then the differentiation was initiated by switching to differentiation medium, see Table 3.1.

membranes of the cells and then washed three times with PBS. The cells were then incubated in 10 % goat serum for 1 hour, followed by another 1 hour incubation with diluted antibodies against PPAR γ and adiponectin (1:200 in 10 % goat serum) in 37 °C. The cells were then rinsed in 1 % goat serum by shaking for 10 minutes, repeated three times. It was crucial to perform the rest of the experiment in darkness, as to not bleach the marker on the secondary antibody. The diluted secondary antibodies (1:200 in 10 % goat serum) were then added at 100 μ l and an incubation for 2 hours in darkness followed. The cells were then rinsed in 1 % goat serum by shaking for 10 minutes, repeated three times. 200 μ l 4',6-diamidino-2-phenylindole (DAPI) (Roche, Switzerland) diluted in PBS (1:5) was added followed by incubation for 10 minutes. Lastly, a washing step with PBS was performed three times and the plate was stored foiled until imaged in a confocal spectroscopy (LSM 780 AxioObserver, Zeiss, Germany).

3.2.1.2 Oil Red O

Adipogenic induced hMSCs, exposed to 0, 10, 100 and 500 μ g/ml particles, were stained with Oil Red O on day 14 after adipogenic induction, to determine the size of the accumulated lipid droplets. The cells were fixed with 4 % (w/v) paraformaldehyde for 30 minutes and then stained by adding 3 vol of Oil Red O 0.5 % and 2 vol of deionized water, incubating for 30 minutes at 37 °C. After rinsing twice with distilled water, the cells were observed using a phase-contrast microscope (Leica, Germany). To quantify the results, the dye was dissolved with isopropanol followed by a measurement of OD at 517 nm using a multimode plate reader (EnSpire, PerkinElmer, USA). Figure 3.2 shows a staining with this protocol performed at the same laboratory as this master thesis was performed.

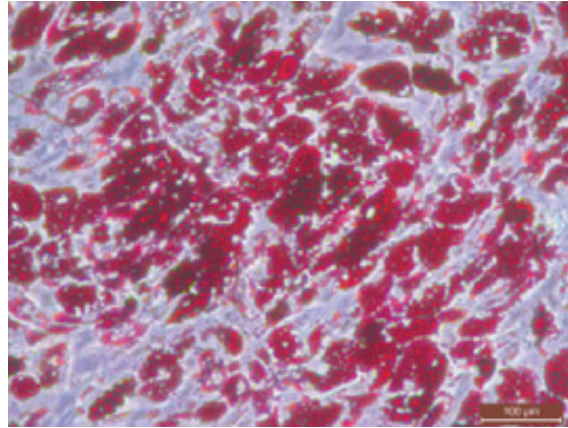


Figure 3.2: A staining with Oil Red O from previous studies performed by He et al. (2016). Length of scale bar is 100 μm .

3.2.1.3 Adiponectin secretion

The secreted proteins of adipogenic induced hMSCs that had been exposed to 10, 50, 100, 250 and 500 $\mu\text{g}/\text{ml}$ PLGA nanoparticles was collected on day 7, 14 and 19 after particle exposure. The cell serum was immediately frozen at $-80\text{ }^{\circ}\text{C}$. Each concentration of exposure was done in duplicate wells on the same plate ($n = 2$). Before measuring the amount of secreted adiponectin, the medium was thawed and centrifuged at 3000 rpm for 20 minutes. Finally, the supernatant was then analysed using a Human Adiponectin Enzyme-Linked Immunosorbent Assay (HAELISA) (Cusabio, China) according to the manufacturer's instructions.

3.3 Statistics

To determine the statistical significance, Student's t-test was used and a p-value of less than 0.05 was deemed as significant (Devore 2012).

4

Results

4.1 Particle characterisation

To determine the hydrodynamic diameter of the PLGA nanoparticles, DLS measurements were performed. The particles were dispersed in deionized water and growth medium without and with FBS, results shown in Figure 4.1, Figure 4.2 and Figure 4.3 respectively. A significant difference was determined between water and the two other samples but not between medium with and without FBS. The calculated yield was 46 %.

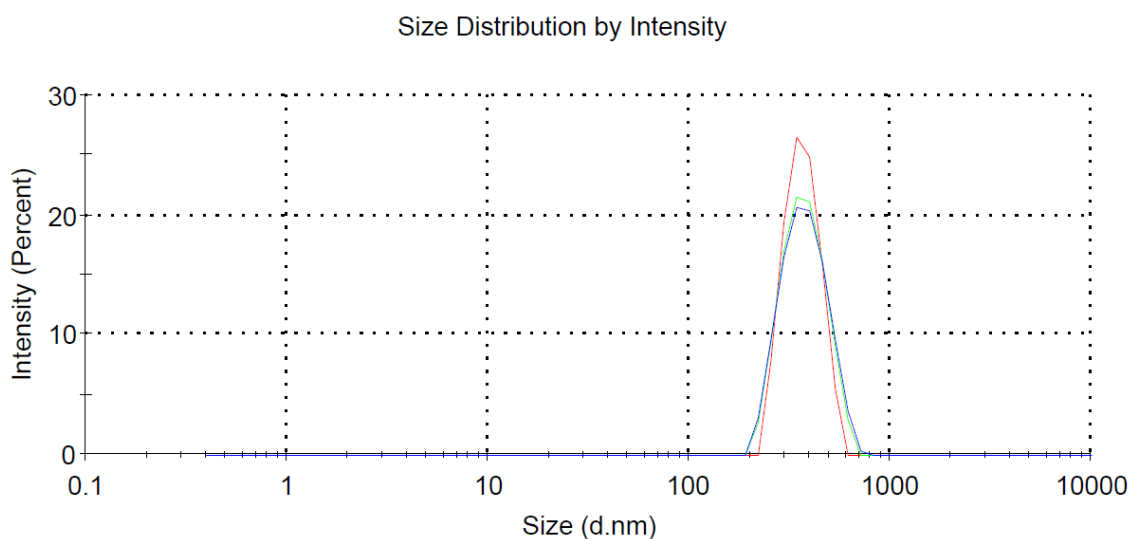


Figure 4.1: DLS measurements of PLGA particles in water. Three repeats in deionized water, order of repeat was red, green then blue. Average diameter of 357.3 nm (Poly-dispersive Index (PdI) = 0.067). Peak at 381.3 (SD = 97.19).

After sterilisation, another DLS measurement was performed to evaluate the effect of γ irradiation on the PLGA particle stability in growth medium. Figure 4.4 shows an unstable particle solution with both small and large particles, with a high PdI. This indicates that the stability of the particles has been compromised during the sterilisation process.

ζ potential was measured to evaluate long term storage stability and risk of aggregation of the particles. Figure 4.5 implies that the net charge is close to zero and

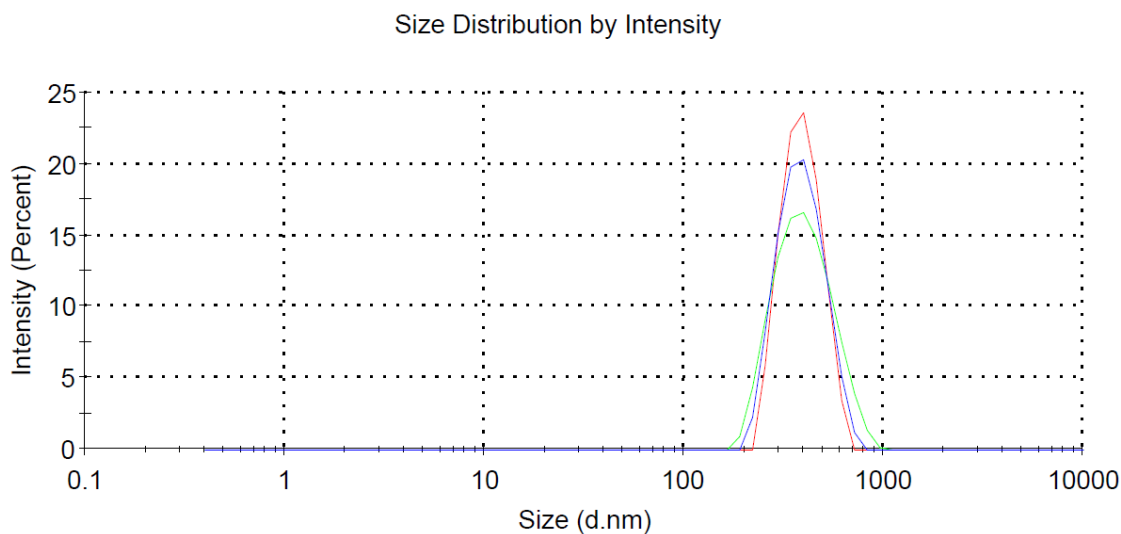


Figure 4.2: DLS measurements of PLGA particles in growth medium. Three repeats in complete growth medium, order of repeat was red, green then blue. Average diameter of 372.1 nm (PdI = 0.103). Peak at 395.0 nm (SD = 104.1).

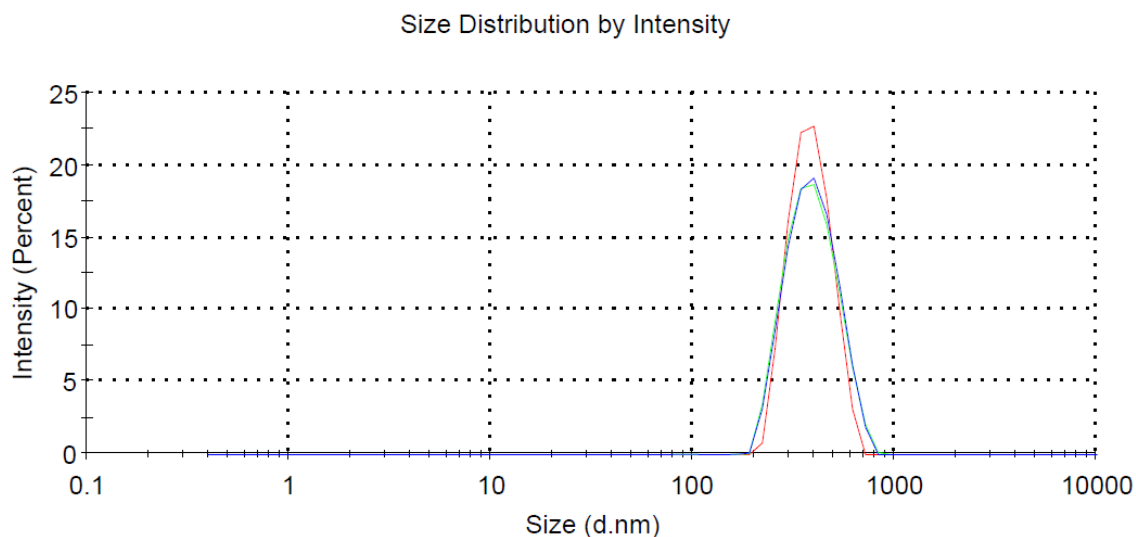


Figure 4.3: DLS measurements of PLGA particles in growth medium with FBS. Three repeats in complete growth medium, order of repeat was red, green then blue. Average diameter of 371.9 nm (PdI = 0.053). Peak at 399.5 (SD = 111.2).

would mean that the risk of aggregation is high due to no inter-particle repellation.

The qualitative images from the SEM, below in Figure 4.6, shows the PLGA particles in three different magnification settings; 10, 25 and 50 kx. Figure 4.6a indicates that the particles have low PdI, supporting the DLS measurements of Figure 4.3. In Figure 4.6b the spherical nature of the particles was confirmed, but with some surface abnormalities. These artifacts are further illustrated in Figure 4.6c, in which the interconnections are visible as well.

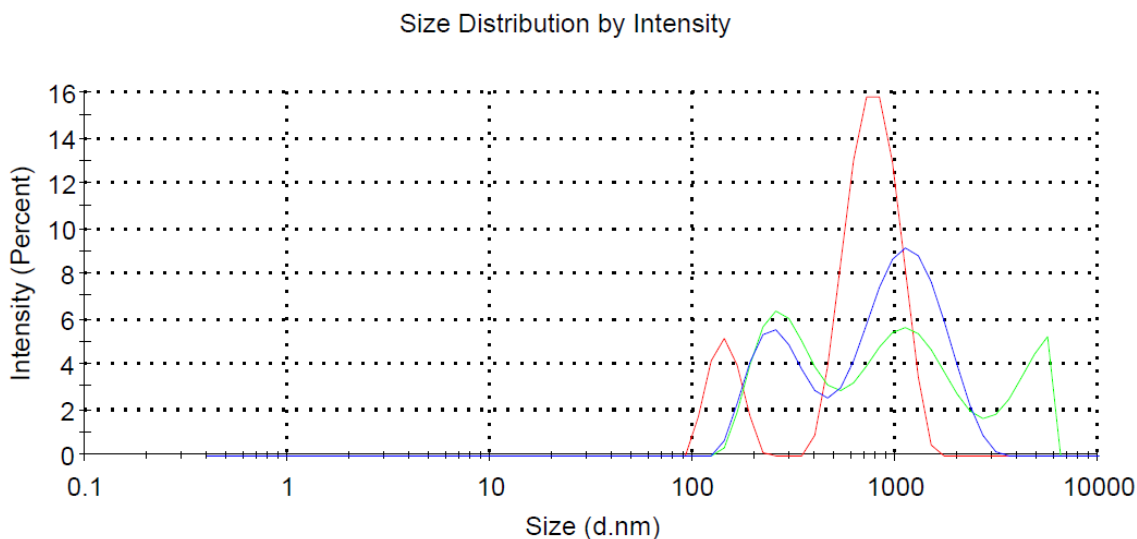


Figure 4.4: DLS measurement of γ irradiated PLGA particles. Three repeats in complete growth medium, order of repeat was red, green then blue. Average diameter of 541.9 (PDI = 0.517). Peaks at 1177 nm (SD = 494.5, 68.7 %) and 277.3 nm (SD = 85.55, 31.3 %).

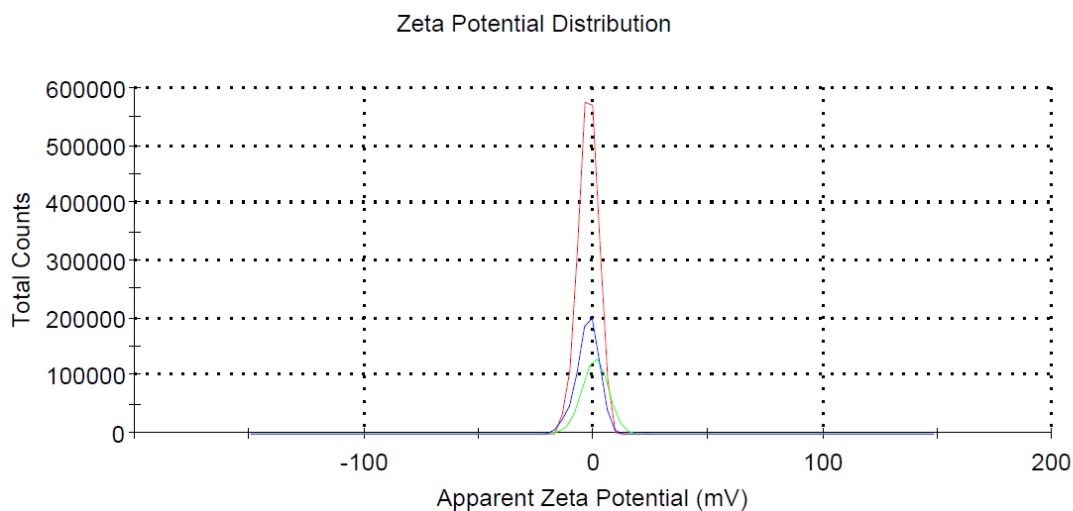


Figure 4.5: Shows the measured ζ potential of the particles. Average of -2.61 mV (SD = 4.97) indicates of low-to-no charge, increasing the risk of aggregation over time.

During the PLGA particle setup, the particles often smelted together. Through a step-wise change of the parameters, such as PVA hydrolysis, polymer concentration, emulsifier type and concentration, ultrasonication effect and time, the problem was found out to be the sputtering. Figure 4.7a shows a batch of particles after being sputtered with gold. No separate particles was visible and they are heavily interconnected with the nodes as smelted particles. When sputtering was changed to platinum, Figure 4.7b shows separated and spherical particles with thin interconnections.

4. Results

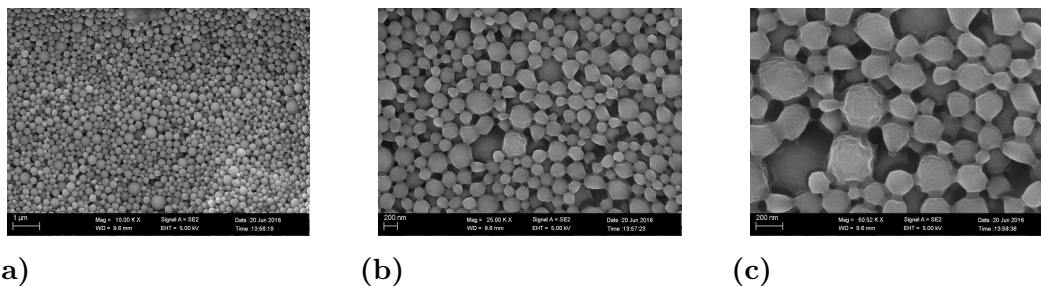


Figure 4.6: SEM pictures of platinum sputtered PLGA nanoparticles, (a) 10k, (b) 25k and (c) 50k magnification.

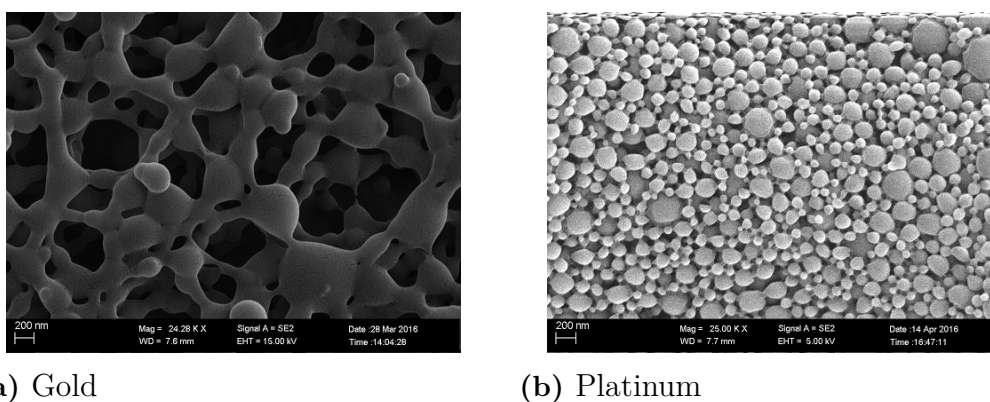


Figure 4.7: The effect of gold vs platinum sputtering on PLGA nanoparticles, 25 kx magnification

Trehalose, a cryoprotectant, was added to the PLGA nanoparticles before freezing. Figure 4.8 shows particles encapsulated in trehalose. The particles are spread out in the trehalose crystal in a monodisperse way, showing single bumps as each particle. The largest particles are >500 nm and the smallest are <100 nm, with most at the size of 200-300 nm.

4.2 Cell culture evaluation

To determine the cytotoxicity of the particles, a CCK-8 was performed at particle concentrations of 10, 50, 100, 250 and 500 $\mu\text{g}/\text{ml}$ (see Figure 4.9). All results were weighted towards the control of Day 1. All samples except 500 $\mu\text{g}/\text{ml}$ had an increase in viable cells from Day 1 to Day 3 followed by a decrease to Day 7, 500 $\mu\text{g}/\text{ml}$ had no statistical change. On Day 1 and 3, all samples were statistically lower than the control, but on Day 7 control decreased and no difference between any sample could be found.

To determine the maturity of the adipocytes, confocal imaging of labeled antibodies for adiponectin and PPAR γ was performed. The results from the adiponectin is

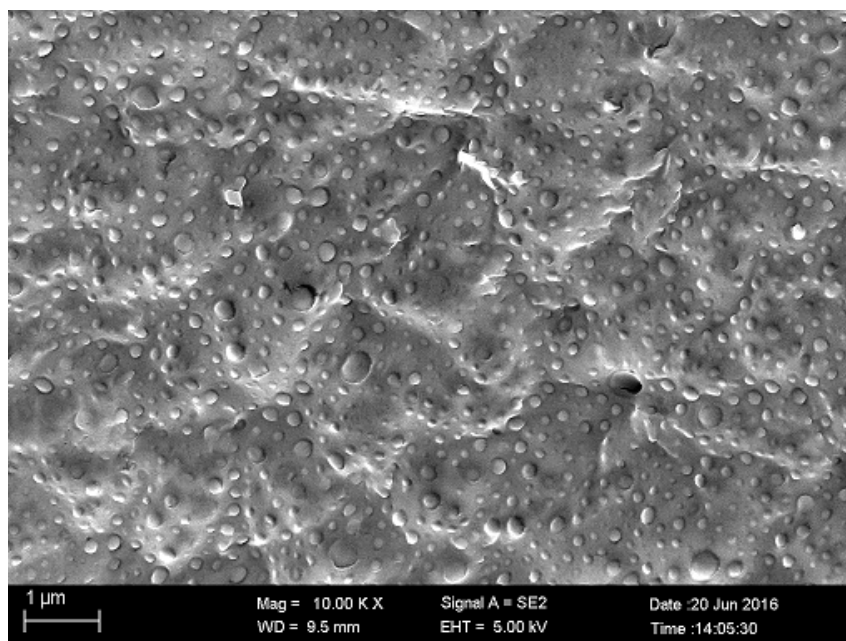


Figure 4.8: SEM images of platinum sputtered PLGA nanoparticles encapsulated in trehalose, 10 kx magnification.

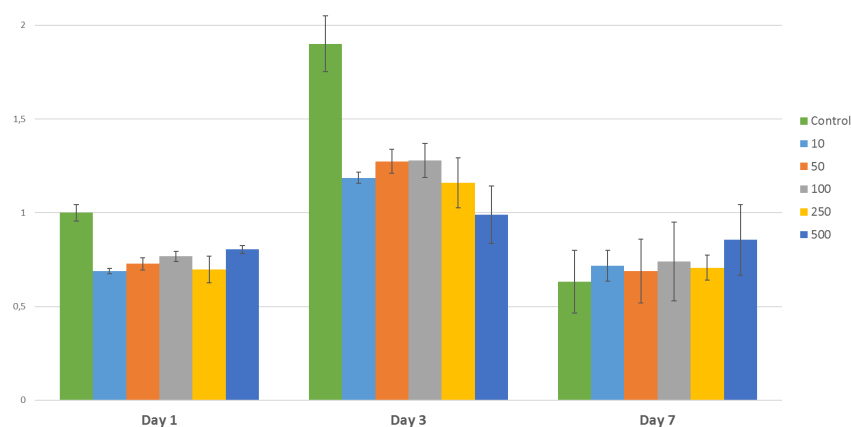


Figure 4.9: CCK8 viability test. Numbers in the legend to the left depict concentrations are of PLGA particles the cells were exposed to on Day 0, y-axis is the absorbance and error bars are standard deviation ($n = 3$). See Table A.1 for the raw data.

visualised in Figure 4.10. The images of adiponectin shows a high live cell count in all except control of differentiation medium and 500 $\mu\text{g}/\text{ml}$ growth medium (Figure 4.10a and Figure 4.10f). All pictures except the high concentration of growth medium have red colouring, indicating of stained adiponectin present.

The results from the confocal microscope when staining for PPAR γ is shown in Figure 4.11. All pictures except the 500 $\mu\text{g}/\text{ml}$ differentiation medium (Figure 4.11c) shows a high live cell concentration. No red colour indicating of no present PPAR γ .

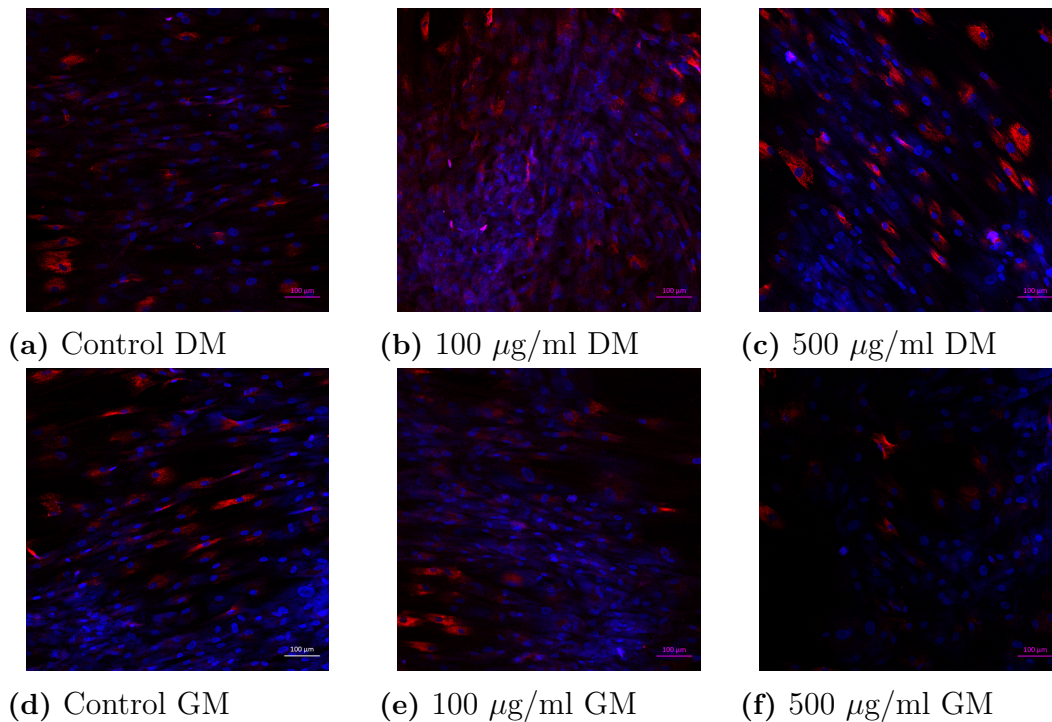


Figure 4.10: Confocal images of immunohistochemistry of expressed adiponectin. Blue colour is DAPI to show the cell nucleus and red colour is the secondary antibody labeled with Fluor 594.

To quantify the secreted adiponectin, a HAELISA kit was used. The result is depicted in Figure 4.12, showing that no cells secreted any detectable level of adiponectin. The two bars on the right shows the absorbance of the two lowest concentrations in the standard, with 0 and 1.5625 ng/ml adiponectin.

Typically for adipocytes, the lipid droplets are few in numbers and covers most of the cell volume, see Figure 3.2. However, the results from the Oil Red O staining, seen below in Figure 4.13, shows mostly small red dots with once exception of Figure 4.13c. Since no live/dead stain is incorporated into the test, the status of the cells are unknown. The outlines might be the footprint of dead cells, and the small red dots might then be necrotic bodies which contains the neutral fats that should have been stored inside the droplets.

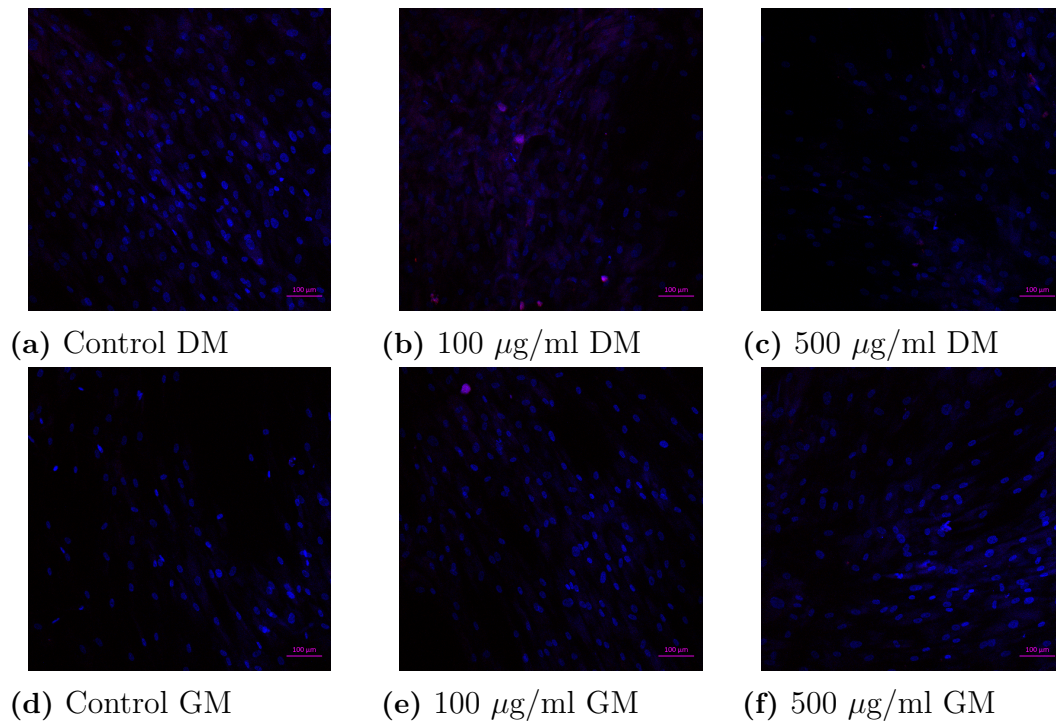


Figure 4.11: Confocal images of immunohistochemistry of PPAR γ . Blue colour is DAPI to show the cell nucleus and red colour is PPAR γ secondary antibody labeled with TRITC.

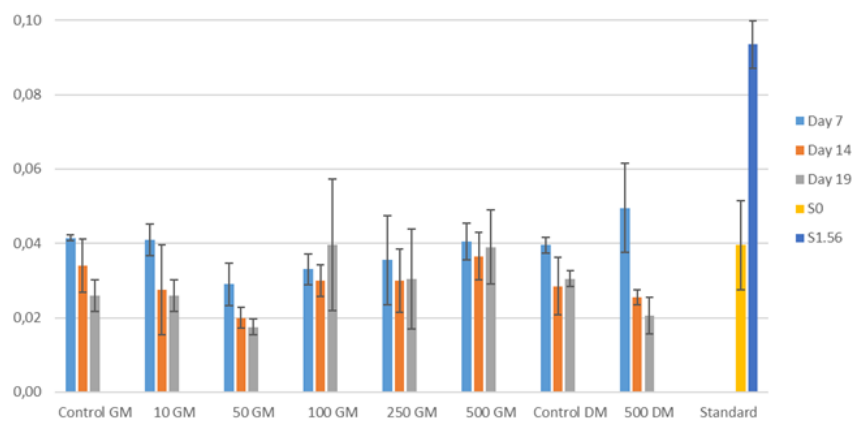
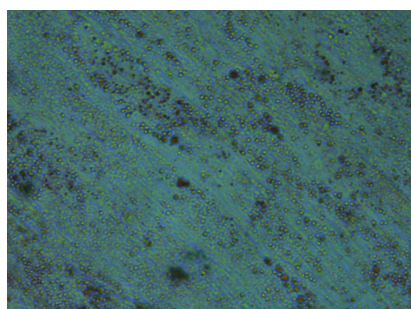
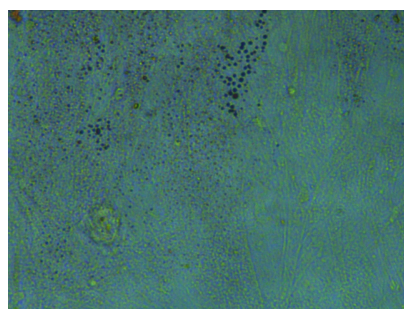


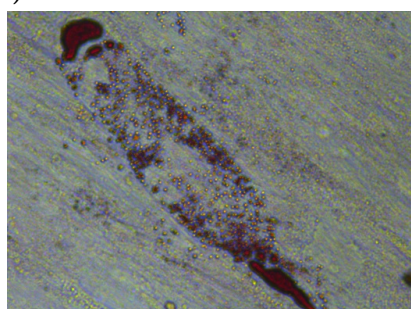
Figure 4.12: Quantitative study of secreted adiponectin. The number indicates the particle concentration in $\mu\text{g/ml}$. S0 is the standard curve measurement without protein, S1.56 has 1.5625 ng/ml adiponectin. See Table A.2 for the raw data.



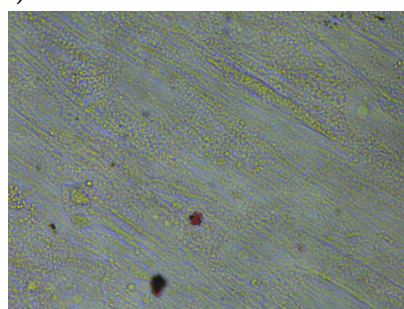
(a) Control DM



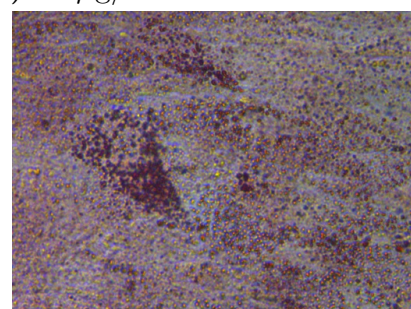
(b) Control GM



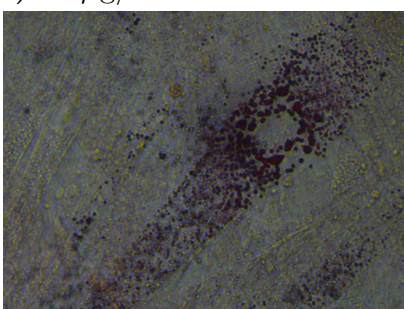
(c) 10 $\mu\text{g/ml}$ DM



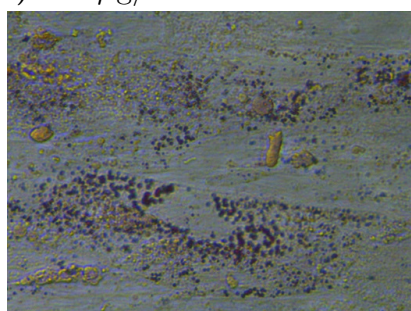
(d) 10 $\mu\text{g/ml}$ GM



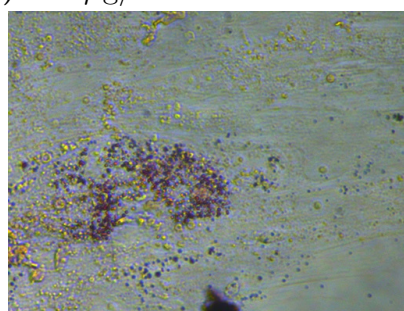
(e) 100 $\mu\text{g/ml}$ DM



(f) 100 $\mu\text{g/ml}$ GM



(g) 500 $\mu\text{g/ml}$ DM



(h) 500 $\mu\text{g/ml}$ GM

Figure 4.13: Oil Red O staining of the fat droplets, 40x magnification. DM stands for differentiation medium, GM stands for growth medium, see Table 3.1 for more information.

5

Discussion

5.1 Particle characterisation

The most time consuming part of this master thesis was the synthesis of the PLGA nanoparticles. The particles seemed to melt together (Figure 4.7a) and a step-wise change of parameters were performed. First it was theorised to be the particle synthesis that introduced too much heat, or that the emulsifiers weren't stable enough or that the melting occurred due to physical forces from centrifuging. However, later on it was discovered to be the gold sputtering that was performed before imaging with SEM. Gold sputtering has previously been used on PLGA with good results, but the sputtering parameters are unknown (Cartiera et al. 2009). Sputtering with platinum requires less energy which creates less heat saved the particles (Figure 4.7b), but the time of exposure varied and sputtering technique might have varied as well (Stuart 1983). After the successful sputtering, the particles still had a rugged surface with thin interconnections (Figure 4.6c) which might be due to small heat exposure during sputtering.

The increase in the hydrodynamic radius of the PLGA nanoparticles between the pure water (Figure 4.1) and medium (Figure 4.2) in the DLS measurements can be explained by the presence of ions. These ions increase the hydrodynamic radius of the PLGA nanoparticle as described in the Theory-chapter, but when comparing to complete medium (Figure 4.3) there is no increase due to protein adsorption. This might be explained by the low ζ potential that was measured (Figure 4.5) which limits the ionic interaction between the particles and the proteins present in the FBS solution (Platel et al. 2016). The limited ionic interaction might inhibit the adsorption of protein on to the surface of the PLGA nanoparticles. When comparing the quantitative size measurements of the DLS to the qualitative measurement of the SEM in Figure 4.6 and Figure 4.8 it is visible that the general size distribution of the PLGA nanoparticles is the same. However, the results from Figure 4.8 can be misleading since different parts of the PLGA nanoparticles might be shown, and some might be completely hidden in the trehalose. The comparison was also only done through visual determination and no quantification of the SEM picture was done.

The low ζ potential (Figure 4.5) indicates that particles aggregate when in suspension, which might affect the cellular uptake efficiency as well as reduce shelf life. When comparing DLS measurements before and after sterilisation (Figure 4.4), the

particles seem to disintegrate and aggregate. The first run (red) shows two peaks, one smaller and one larger than 350 nm. The green run (second) shows a further increased size for all peaks, and newly formed microspheres above 4 μm . The largest peak then disappears in the third run (blue). This might be either from sedimentation or that the larger particles keep aggregating and gets too big for the DLS measurement to detect. The aggregation of PLGA nanoparticles concurs with the results from the ζ potential measurements (Figure 4.5), where a low ζ potential allows for rapid aggregation due to no inter-particle repulsion present. The reason for this apparent damage of the PLGA nanoparticles might be the γ irradiation. This method introduces heat, the amount depending on the exact sterilisation protocol. Previous work has been able to sterilise with γ rays at 25 kGy, indicating that the method during this thesis is suboptimal (Bozdag et al. 2005). The DLS measurements performed by Bozdag et al. (2005) was done with only ions present limiting the exact correlation between this thesis' and their results.

Furthermore, the PLGA nanoparticles that were exposed to the cells were all sterilised. The results from Figure 4.4 then indicates that the actual size of these particles were not monodispersed and ~ 350 nm as proposed by the non-sterilised DLS measurement, but rather a mix of both large and small aggregates of the fragments of nanoparticles. The sterilising γ rays can cause polymer cross-linking breakage which might fragment the particles (Lü et al. 2009). The fragments might then aggregate easier but it is hard to estimate since no ζ potential measurement was performed on any sterilised particles. However, Bozdag et al. (2005) managed to sterilise PLGA nanoparticles without any significant effect on neither hydrodynamic radius nor ζ potential. This indicates that the particles produced during this thesis might have had irregularities when comparing to current knowledge, but no explanation can be found.

5.2 Cell culture evaluation

The CCK8 viability test shows (see Figure 4.9) an early cell cytotoxicity, but the control on Day 7 indicates that something has happened and it is therefore excluded from any conclusion. This demonstrates of a cytotoxicity even at low particle concentration, which might limit any future applicability of them as drug delivery vectors. This was somewhat expected due to the size dependant cytotoxicity found by previous studies, although at smaller sizes (Xiong et al. 2013). The PLGA nanoparticles induces cellular damage through several mechanisms, including ROS generation and inflammatory reaction. The findings by Xiong et al. (2013) indicates that there is an optimal size when weighing the increased cellular uptake as well as cytotoxicity as the particles get smaller. By coating the particles with e.g. chitosan, the cytotoxicity might diminish. This would allow for small non-toxic PLGA nanoparticles with a high efficiency of cellular uptake.

The qualitative test of PPAR γ shows little-to-no expression in the cells, even after exposure to the differentiation medium (Figure 4.11). This indicates of no adipocytes,

but quantitative a measurement of a plate reader or PCR of related gene expression would have been required to get a proper conclusion. The confocal images of adiponectin shows expression of the gene in the control which indicates mishandling of the sample, such as high exposure which would show background staining and thereby show a false-positive (Figure 4.10). The quantitative test of secreted adiponectin exhibit no secretion of the protein in any sample, further strengthening the conclusion of no adult adipocytes present.

The differentiation method was based on the work of He et al. (2016), with two significant differences. The first, and most significant, difference was that He et al. (2016) repeated the differentiation/induction cycle three times whereas the method in this thesis only did it once. The second difference was that the incubation time on the differentiation medium was three days and the induction only one day, where the method applied differentiation medium for two days and then induction medium for the remainder of the experiment. This would inhibit the hMSCs from fully differentiating to adipocytes since they would get stuck in a preadipocyte without the presence of any differentiating markers. This would explain the lack of mature adipocytes. The reason behind this was to determine of the increased ROS generation, which activates expression of PPAR γ , from PLGA nanoparticles was large enough to keep the differentiation going once started (Tormos et al. 2011). However, no positive control was included in the experiment, limiting the significance of the findings.

Given the increased ROS generation that PLGA nanoparticles seem to have in hMSCs, the differentiation towards was expected to be increased (Xiong et al. 2013). The ROS would increase the PPAR γ expression which in turn would differentiate the cells towards adipocytes (Otto & Lane 2005). The expressed PPAR γ would also be visible in the confocal images of the protein in Figure 4.11. Since no expression is seen, the amount of ROS might be lower then previous studies. This would be inconsistent with current knowledge about PLGA nanoparticles and further studies in the produced nanoparticles might be of interest.

The Oil Red O staining shows of small red dots, instead of the large bubbles adult adipocytes have (He et al. 2016). This might be smaller cellular compartments with neutral fats inside, which would indicate of a preadipocyte (see Figure 4.13c), or cross staining of other cell compartments or PLGA nanoparticles. Figure 4.13g also shows of unidentified yellow particles. These are not stained by the Oil Red O and is unlikely to be fat droplets, but might be larger aggregation of particles. The undifferentiated cells with particle exposure (Figure 4.13f) shows of the same small stained dots, indicating that they are not from the adipogenesis. Another explanation to the lack of lipid droplets might also be that the cells are dead. The small red dots might then be the leftovers of an adipocyte that has gone through necrosis or apoptosis. Since only a few pictures was taken, and neither contained any staining for live cells, it is not possible to determine the reason behind any cell death. Previous work with the same protocol performed by He et al. (2016) investigated the effect of silver nanoparticles on adipogenesis. The cells seen in Figure 3.2 was sub-

jected to the same differentiation medium, although with a different schedule (see above). This allowed the cells of He et al. (2016) to fully differentiate into mature adipocytes with the large fat droplets. The small dots in Figure 4.13 shows that the modified protocol failed to produce any live mature adipocytes.

5.3 Future

The PLGA nanoparticles that was produced during this thesis seemed to be less stable then what previous studies suggests. Previous studies has been able to sterilise PLGA nanoparticles with 25 kGy γ irradiation, which is higher than used in the proposed method. No clear explanation can be found and deeper analysis of the physicochemical properties of the bought polymer might be needed. Determining the glass transition temperature might give a clue as to why gold sputtering melted the particles as well.

To continue the research present on the cytotoxicity, future studies could monitor ROS generation and/or inflammatory cytokines (such as TNF- α) while determining the cell viability from a wider range of particle sizes. This would allow for scientists to find the optimal ratio between cellular uptake for drug delivery efficiency without too high adverse effects.

During cellular uptake, the cells do not interact directly with the particles but rather to the biofilm that macromolecules (such as proteins) and ions form when the PLGA nanoparticles are in the complete medium. This makes the findings when comparing the DLS measurements of Figure 4.2 and Figure 4.3 interesting to look further into. When comparing coated to non-coated PLGA nanoparticles, the coating seem to decrease cytotoxicity which might be due to a changed adsorption profile on the surface. Future studies should determine if the non-difference in size is consistent over time as well as try to determine how the surface coating affects the adsorption profile. Further on, determining where in the cell the PLGA nanoparticles end up might be crucial to understand as to what kind of drug it can deliver. Internalisation evaluations such as transmission electron microscope with marker-loaded particles would illuminate this.

6

Conclusion

PLGA nanoparticles with a size of approximately 350 nm have been produced with a single emulsification-solvent evaporation protocol, small enough for pinocytosis for adipocytes. The synthesised particles were monodispersed and spherical, but the low yield of 46 % makes the protocol unsuitable for larger production scale. The type of metal used in the sputter proved to be crucial. Figure 4.7 shows that the gold sputtering approach introduced too much heat and the particles subsequently melted. Using platinum kept the particles intact and separated. The SEM images indicated of an effective encapsulation of trehalose, and thereby an effective cryoprotectant. However, after the γ irradiation the DLS measurements indicates of a disintegration.

The CCK-8 test indicate of an early cytotoxic effect of the PLGA nanoparticles. The evaluation of the effect of PLGA nanoparticles on the adipogenic differentiation was inconclusive. The confocal images of the PPAR γ and adiponectin show staining in the control, indicating of a failed experiment or imaging. The amount of secreted adiponectin was not statistically different from the 0 ng/ml in the standard, suggesting of no present adipocyte. The proposed protocol was concluded to be unsuccessful at differentiating hMSCs into mature adipocytes.

Microscope pictures of the stained lipid droplets show small, red dots which might be either small fat droplets of immature adipocytes, footprints of dead cells or cross staining of the PLGA nanoparticles aggregates.

Bibliography

- Abdelwahed, W., Degobert, G., Stainmesse, S. & Fessi, H. (2006), 'Freeze-drying of nanoparticles: Formulation, process and storage considerations', *Advanced Drug Delivery Reviews* **58**(15), 1688 – 1713. 2006 Supplementary Non-Thematic Collection.
- URL:** <http://www.sciencedirect.com/science/article/pii/S0169409X06001840>
- Anderson, J. M. & Shive, M. S. (2012), 'Biodegradation and biocompatibility of plga and plga microspheres', *Advanced drug delivery reviews* **64**, 72–82.
- Anderson, J. W., Konz, E. C., Frederich, R. C. & Wood, C. L. (2001), 'Long-term weight-loss maintenance: a meta-analysis of us studies', *The American journal of clinical nutrition* **74**(5), 579–584.
- Astete, C. E. & Sabliov, C. M. (2006), 'Synthesis and characterization of plga nanoparticles', *Journal of Biomaterials Science, Polymer Edition* **17**(3), 247–289.
- Berne, B. J. & Pecora, R. (2000), *Dynamic light scattering: with applications to chemistry, biology, and physics*, Courier Corporation.
- Bjorbæk, C. & Kahn, B. B. (2004), 'Leptin signaling in the central nervous system and the periphery', *Recent progress in hormone research* **59**, 305–332.
- Bowers, R. R. & Lane, M. D. (2007), 'A role for bone morphogenetic protein-4 in adipocyte development', *Cell Cycle* **6**(4), 385–389.
- Bozdog, S., Dillen, K., Vandervoort, J. & Ludwig, A. (2005), 'The effect of freeze-drying with different cryoprotectants and gamma-irradiation sterilization on the characteristics of ciprofloxacin hcl-loaded poly (d, l-lactide-glycolide) nanoparticles', *Journal of pharmacy and pharmacology* **57**(6), 699–707.
- Buchwald, H., Avidor, Y., Braunwald, E., Jensen, M. D., Pories, W., Fahrbach, K. & Schoelles, K. (2004), 'Bariatric surgery: a systematic review and meta-analysis', *Jama* **292**(14), 1724–1737.
- Cartiera, M. S., Johnson, K. M., Rajendran, V., Caplan, M. J. & Saltzman, W. M. (2009), 'The uptake and intracellular fate of plga nanoparticles in epithelial cells', *Biomaterials* **30**(14), 2790–2798.
- Chandran, M., Phillips, S. A., Ciaraldi, T. & Henry, R. R. (2003), 'Adiponectin: more than just another fat cell hormone?', *Diabetes care* **26**(8), 2442–2450.

- Dechy-Cabaret, O., Martin-Vaca, B. & Bourissou, D. (2004), 'Controlled ring-opening polymerization of lactide and glycolide', *Chemical reviews* **104**(12), 6147–6176.
- Devore, J. L. (2012), *Probability and Statistics for Engineering and the Sciences*, Vol. 8, Cengage Learning.
- Diez, J. J. & Iglesias, P. (2003), 'The role of the novel adipocyte-derived hormone adiponectin in human disease', *European Journal of endocrinology* **148**(3), 293–300.
- Dillen, K., Vandervoort, J., den Mooter, G. V., Verheyden, L. & Ludwig, A. (2004), 'Factorial design, physicochemical characterisation and activity of ciprofloxacin-plga nanoparticles', *International Journal of Pharmaceutics* **275**(1–2), 171 – 187.
URL: <http://www.sciencedirect.com/science/article/pii/S0378517304000687>
- Dojindo (2016), 'Cell counting kit-8 technical manual'. https://www.dojindo.com/TechnicalManual/Manual_CK04.pdf [Accessed 2017-04-18].
- Dunne, M., Corrigan, O. & Ramtoola, Z. (2000), 'Influence of particle size and dissolution conditions on the degradation properties of polylactide-co-glycolide particles', *Biomaterials* **21**(16), 1659 – 1668.
URL: <http://www.sciencedirect.com/science/article/pii/S0142961200000405>
- Fahmy, T. M., Samstein, R. M., Harness, C. C. & Saltzman, W. M. (2005), 'Surface modification of biodegradable polyesters with fatty acid conjugates for improved drug targeting', *Biomaterials* **26**(28), 5727–5736.
- Fain, J. N., Madan, A. K., Hiler, M. L., Cheema, P. & Bahouth, S. W. (2004), 'Comparison of the release of adipokines by adipose tissue, adipose tissue matrix, and adipocytes from visceral and subcutaneous abdominal adipose tissues of obese humans', *Endocrinology* **145**(5), 2273–2282.
- Feve, B. (2005), 'Adipogenesis: cellular and molecular aspects', *Best Practice & Research Clinical Endocrinology & Metabolism* **19**(4), 483–499.
- Fishbein, I., Chorny, M., Banai, S., Levitzki, A., Danenberg, H. D., Gao, J., Chen, X., Moerman, E., Gati, I., Goldwasser, V. et al. (2001), 'Formulation and delivery mode affect disposition and activity of tyrphostin-loaded nanoparticles in the rat carotid model', *Arteriosclerosis, thrombosis, and vascular biology* **21**(9), 1434–1439.
- Fröhlich, E. (2012), 'The role of surface charge in cellular uptake and cytotoxicity of medical nanoparticles', *Int J Nanomedicine* **7**(1), 5577–91.
- Fröhlich, E., Meindl, C., Roblegg, E., Griesbacher, A. & Pieber, T. R. (2012), 'Cytotoxicity of nanoparticles is influenced by size, proliferation and embryonic origin of the cells used for testing', *Nanotoxicology* **6**(4), 424–439.
- Gentile, P., Chiono, V., Carmagnola, I. & Hatton, P. V. (2014), 'An overview of poly (lactic-co-glycolic) acid (plga)-based biomaterials for bone tissue engineering', *International journal of molecular sciences* **15**(3), 3640–3659.

- Green, H. & Kehinde, O. (1975), 'An established preadipose cell line and its differentiation in culture ii. factors affecting the adipose conversion', *Cell* **5**(1), 19–27.
- Gunatillake, P. A. & Adhikari, R. (2003), 'Biodegradable synthetic polymers for tissue engineering', *Eur Cell Mater* **5**(1), 1–16.
- Hammond, R. A. & Levine, R. (2010), 'The economic impact of obesity in the united states', *Diabetes Metab Syndr Obes* **3**(1), 285–95.
- He, W., Elkhooly, T. A., Liu, X., Cavallaro, A., Taheri, S., Vasilev, K. & Feng, Q. (2016), 'Silver nanoparticle based coatings enhance adipogenesis compared to osteogenesis in human mesenchymal stem cells through oxidative stress', *Journal of Materials Chemistry B* **4**(8), 1466–1479.
- Holzer, M., Vogel, V., Mäntele, W., Schwartz, D., Haase, W. & Langer, K. (2009), 'Physico-chemical characterisation of {PLGA} nanoparticles after freeze-drying and storage', *European Journal of Pharmaceutics and Biopharmaceutics* **72**(2), 428 – 437. Special Section: Biological Barriers and Nanomedicine- Advanced Drug Delivery and Predictive non vivo Testing Technologies.
URL: <http://www.sciencedirect.com/science/article/pii/S0939641109000563>
- Hooper, K. A., Cox, J. D. & Kohn, J. (1997), 'Comparison of the effect of ethylene oxide and γ -irradiation on selected tyrosine-derived polycarbonates and poly (l-lactic acid)', *Journal of applied polymer science* **63**(11), 1499–1510.
- Jiang, P., Yu, D., Zhang, W., Mao, Z. & Gao, C. (2015), 'Influence of bovine serum albumin coated poly (lactic-co-glycolic acid) particles on differentiation of mesenchymal stem cells', *RSC Advances* **5**(51), 40924–40931.
- Kanda, Y., Hinata, T., Kang, S. W. & Watanabe, Y. (2011), 'Reactive oxygen species mediate adipocyte differentiation in mesenchymal stem cells', *Life sciences* **89**(7), 250–258.
- Kern, P. A., Di Gregorio, G. B., Lu, T., Rassouli, N. & Ranganathan, G. (2003), 'Adiponectin expression from human adipose tissue', *Diabetes* **52**(7), 1779–1785.
- Khursheed, A. (2011), *Scanning electron microscope optics and spectrometers*, World scientific.
- Kinlaw, W. B. & Marsh, B. (2004), 'Adiponectin and hiv-lipodystrophy: taking haart', *Endocrinology* **145**(2), 484–486.
- Kohane, D. S. (2007), 'Microparticles and nanoparticles for drug delivery', *Biotechnology and bioengineering* **96**(2), 203–209.
- Kowalski, A., Duda, A. & Penczek, S. (2000), 'Mechanism of cyclic ester polymerization initiated with tin (ii) octoate. 2. macromolecules fitted with tin (ii) alkoxide species observed directly in maldi-tof spectra', *Macromolecules* **33**(3), 689–695.
- Kricheldorf, H. R., Boettcher, C. & Tönnies, K.-U. (1992), 'Polylactones: 23. polymerization of racemic and meso, l-lactide with various organotin catalysts—stereochemical aspects', *Polymer* **33**(13), 2817–2824.

- Li, J., Stayshich, R. M. & Meyer, T. Y. (2011), 'Exploiting sequence to control the hydrolysis behavior of biodegradable plga copolymers', *Journal of the American Chemical Society* **133**(18), 6910–6913.
- Li, S. & Vert, M. (2002), Biodegradation of aliphatic polyesters, *in* 'Degradable polymers', Springer, pp. 71–131.
- Lord, G. M., Matarese, G., Howard, J. K., Baker, R. J., Bloom, S. R. & Lechler, R. I. (1998), 'Leptin modulates the t-cell immune response and reverses starvation-induced immunosuppression', *Nature* **394**(6696), 897–901.
- Lü, J.-M., Wang, X., Marin-Muller, C., Wang, H., Lin, P. H., Yao, Q. & Chen, C. (2009), 'Current advances in research and clinical applications of plga-based nanotechnology', *Expert review of molecular diagnostics* **9**(4), 325–341.
- Malvern.com (2017), 'Zeta potential'. <http://www.malvern.com/en/products/measurement-type/zeta-potential/default.aspx> [Accessed 2017-05-17].
- Margetic, S., Gazzola, C., Pegg, G. & Hill, R. (2002), 'Leptin: a review of its peripheral actions and interactions.', *International Journal of Obesity & Related Metabolic Disorders* **26**(11).
- Mendes, G. C., Brandao, T. R. & Silva, C. L. (2007), 'Ethylene oxide sterilization of medical devices: a review', *American journal of infection control* **35**(9), 574–581.
- Müller, M., Vörös, J., Csucs, G., Walter, E., Danuser, G., Merkle, H., Spencer, N. & Textor, M. (2003), 'Surface modification of plga microspheres', *Journal of Biomedical Materials Research Part A* **66**(1), 55–61.
- Mura, S., Hillaireau, H., Nicolas, J., Le Droumaguet, B., Gueutin, C., Zanna, S., Tsapis, N. & Fattal, E. (2011), 'Influence of surface charge on the potential toxicity of plga nanoparticles towards calu-3 cells', *International journal of nanomedicine* **6**, 2591.
- Ng, M., Fleming, T., Robinson, M., Thomson, B., Graetz, N., Margono, C., Mullany, E. C., Biryukov, S., Abbafati, C., Abera, S. F. et al. (2014), 'Global, regional, and national prevalence of overweight and obesity in children and adults during 1980–2013: a systematic analysis for the global burden of disease study 2013', *The Lancet* **384**(9945), 766–781.
- Nuttall, M. E., Singh, V., Thomas-Porch, C., Frazier, T., Gimble, J. M. et al. (2014), 'Adipocytes and the regulation of bone remodeling: a balancing act', *Calcified tissue international* **94**(1), 78–87.
- O'Brien, P. E., MacDonald, L., Anderson, M., Brennan, L. & Brown, W. A. (2013), 'Long-term outcomes after bariatric surgery: fifteen-year follow-up of adjustable gastric banding and a systematic review of the bariatric surgical literature', *Annals of surgery* **257**(1), 87–94.
- Otto, T. C. & Lane, M. D. (2005), 'Adipose development: from stem cell to adipocyte', *Critical reviews in biochemistry and molecular biology* **40**(4), 229–242.

- Panyam, J. & Labhasetwar, V. (2003), 'Biodegradable nanoparticles for drug and gene delivery to cells and tissue', *Advanced drug delivery reviews* **55**(3), 329–347.
- Platel, A., Carpentier, R., Becart, E., Mordacq, G., Betbeder, D. & Nessler, F. (2016), 'Influence of the surface charge of plga nanoparticles on their in vitro genotoxicity, cytotoxicity, ros production and endocytosis', *Journal of Applied Toxicology* **36**(3), 434–444.
- Pories, W. J. (2008), 'Bariatric surgery: risks and rewards', *The Journal of Clinical Endocrinology & Metabolism* **93**(11_supplement_1), s89–s96.
- Qiang, L., Wang, H. & Farmer, S. R. (2007), 'Adiponectin secretion is regulated by sirt1 and the endoplasmic reticulum oxidoreductase ero1- α ', *Molecular and cellular biology* **27**(13), 4698–4707.
- Quintiliani, L. (2007), 'The workplace as a setting for interventions to improve diet and promote physical activity'. <http://www.who.int/dietphysicalactivity/Quintiliani-workplace-as-setting.pdf?ua=1> [Accessed: 2016-11-30].
- Rosen, E. D. & MacDougald, O. A. (2006), 'Adipocyte differentiation from the inside out', *Nature reviews Molecular cell biology* **7**(12), 885–896.
- Sahoo, S. K., Panyam, J., Prabha, S. & Labhasetwar, V. (2002), 'Residual polyvinyl alcohol associated with poly (d, l-lactide-co-glycolide) nanoparticles affects their physical properties and cellular uptake', *Journal of controlled release* **82**(1), 105–114.
- Seale, P., Conroe, H. M., Estall, J., Kajimura, S., Frontini, A., Ishibashi, J., Cohen, P., Cinti, S. & Spiegelman, B. M. (2011), 'Prdm16 determines the thermogenic program of subcutaneous white adipose tissue in mice', *The Journal of clinical investigation* **121**(1), 96–105.
- Singh, N., Manshian, B., Jenkins, G. J., Griffiths, S. M., Williams, P. M., Maffei, T. G., Wright, C. J. & Doak, S. H. (2009), 'Nanogenotoxicology: the dna damaging potential of engineered nanomaterials', *Biomaterials* **30**(23), 3891–3914.
- Smoluchowski, M. v. (1903), 'Contribution to the theory of electro-osmosis and related phenomena', *Bull Int Acad Sci Cracovie* **3**, 184–199.
- Song, K. C., Lee, H. S., Choung, I. Y., Cho, K. I., Ahn, Y. & Choi, E. J. (2006), 'The effect of type of organic phase solvents on the particle size of poly (d, l-lactide-co-glycolide) nanoparticles', *Colloids and Surfaces A: Physicochemical and Engineering Aspects* **276**(1), 162–167.
- Spenlehauer, G., Vert, M., Benoit, J. & Boddart, A. (1989), 'In vitro and in vivo degradation of poly (d, l lactide/glycolide) type microspheres made by solvent evaporation method', *Biomaterials* **10**(8), 557–563.
- Stayshich, R. M. & Meyer, T. Y. (2008), 'Preparation and microstructural analysis of poly (lactic-alt-glycolic acid)', *Journal of Polymer Science Part A: Polymer Chemistry* **46**(14), 4704–4711.

- Stuart, R. (1983), {CHAPTER} {IV} - {SPUTTERING}, in R. Stuart, ed., 'Vacuum Technology, Thin Films, and Sputtering', Academic Press, San Diego, pp. 91 – 135.
URL: <http://www.sciencedirect.com/science/article/pii/B978012674780550007X>
- Tabata, Y. & Ikada, Y. (1988), 'Macrophage phagocytosis of biodegradable microspheres composed of l-lactic acid/glycolic acid homo-and copolymers', *Journal of Biomedical Materials Research Part A* **22**(10), 837–858.
- Taylor, S. M. & Jones, P. A. (1979), 'Multiple new phenotypes induced in 10t12 and 3t3 cells treated with 5-azacytidine', *Cell* **17**(4), 771–779.
- Tormos, K. V., Anso, E., Hamanaka, R. B., Eisenbart, J., Joseph, J., Kalyanaraman, B. & Chandel, N. S. (2011), 'Mitochondrial complex iii ros regulate adipocyte differentiation', *Cell metabolism* **14**(4), 537–544.
- Twells, L. (2015), 'Severe obesity: Health or economics?', *Canadian Journal of Diabetes* **39**, S3.
- Vázquez-Vela, M. E. F., Torres, N. & Tovar, A. R. (2008), 'White adipose tissue as endocrine organ and its role in obesity', *Archives of medical research* **39**(8), 715–728.
- Verma, A. & Stellacci, F. (2010), 'Effect of surface properties on nanoparticle–cell interactions', *Small* **6**(1), 12–21.
- Wajchenberg, B. L. (2000), 'Subcutaneous and visceral adipose tissue: their relation to the metabolic syndrome', *Endocrine reviews* **21**(6), 697–738.
- Wang, Z.-Y., Zhao, Y.-M., Wang, F. & Wang, J. (2006), 'Syntheses of poly (lactic acid-co-glycolic acid) serial biodegradable polymer materials via direct melt polycondensation and their characterization', *Journal of applied polymer science* **99**(1), 244–252.
- WHO (2013), 'Obesity - data and statistics'. <http://www.euro.who.int/en/health-topics/noncommunicable-diseases/obesity/data-and-statistics> [Accessed 2016-11-30].
- Win, K. Y. & Feng, S.-S. (2005), 'Effects of particle size and surface coating on cellular uptake of polymeric nanoparticles for oral delivery of anticancer drugs', *Biomaterials* **26**(15), 2713–2722.
- Wu, J., Boström, P., Sparks, L. M., Ye, L., Choi, J. H., Giang, A.-H., Khandekar, M., Virtanen, K. A., Nuutila, P., Schaart, G. et al. (2012), 'Beige adipocytes are a distinct type of thermogenic fat cell in mouse and human', *Cell* **150**(2), 366–376.
- Xiong, S., George, S., Yu, H., Damoiseaux, R., France, B., Ng, K. W. & Loo, J. S.-C. (2013), 'Size influences the cytotoxicity of poly (lactic-co-glycolic acid)(plga) and titanium dioxide (tio2) nanoparticles', *Archives of toxicology* **87**(6), 1075–1086.
- Yanovski, S. Z. & Yanovski, J. A. (2014), 'Long-term drug treatment for obesity: a systematic and clinical review', *Jama* **311**(1), 74–86.

Zhang, Y., Proenca, R., Maffei, M., Barone, M., Leopold, L. & Friedman, J. M. (1994), 'Positional cloning of the mouse obese gene and its human homologue', *Nature* **372**(6505), 425.

A

Appendices

A.1 Appendix I

	Control	10	50	100	250	500
Day 1	0.966	0.635	0.606	0.673	0.554	0.711
	0.851	0.605	0.653	0.667	0.615	0.711
	0.88	0.612	0.697	0.701	0.605	0.762
	0.916	0.635	0.673	0.735	0.748	0.724
Day 3	1.945	1.117	1.119	1.22	0.953	0.966
	1.738	1.05	1.249	1.235	0.988	0.761
	1.54	1.081	1.159	1.161	0.974	0.738
	1.647	1.04	1.078	1.004	1.279	1.110
Day 7	0.846	0.765	0.769	0.945	0.711	0.655
	0.541	0.674	0.393	0.361	0.66	1.035
	0.498	0.604	0.523	0.735	0.657	0.859
	0.397	0.545	0.804	0.63	0.528	0.541

Table A.1: Raw data from Cell Counting Kit-8 test. Each PLGA particle concentration had 4 repeats.

A.2 Appendix II

Well	MeasA	MeasB	Blanked	Well	MeasA	MeasB	Blanked
A01	0,088	0,04	0,045	A05	0,079	0,04	0,039
A02	0,068	0,037	0,031	A06	0,066	0,037	0,029
B01	0.127	0,038	0,089	B05	0,073	0,037	0,036
B02	0.137	0,039	0,098	B06	0,056	0,037	0,019
C01	0.177	0,039	0.138	C05	0,057	0,039	0,018
C02	0.167	0,038	0.129	C06	0,059	0,037	0,022
D01	0.239	0,041	0.199	D05	0,076	0,043	0,033
D02	0.25	0,042	0.208	D06	0,065	0,038	0,027
E01	0.466	0,044	0.422	E05	0,075	0,039	0,036
E02	0.494	0,045	0.449	E06	0,062	0,038	0,02
F01	0.795	0,048	0.747	F05	0,069	0,037	0,032
F02	0.789	0,046	0.743	F06	0.08	0,039	0,041
G01	1.247	0,051	1.196	G05	0,061	0,038	0,023
G02	1.231	0,048	1.183	G06	0,072	0,038	0,034
H01	1.87	0,059	1.811	H05	0,062	0,038	0,024
H02	1.917	0.06	1.857	H06	0,064	0,037	0,027
A03	0,078	0,037	0,041	A07	0,066	0,037	0,029
A04	0,079	0,037	0,042	A08	0.06	0,037	0,023
B03	0,081	0,037	0,044	B07	0,069	0.04	0,029
B04	0,076	0,038	0,038	B08	0,063	0.04	0,023
C03	0,071	0,038	0,033	C07	0,053	0,037	0,016
C04	0,064	0,039	0,025	C08	0,057	0,038	0,019
D03	0,072	0,042	0,03	D07	0,065	0,038	0,027
D04	0,078	0,042	0,036	D08	0.09	0,038	0,052
E03	0,084	0.04	0,044	E07	0,079	0,039	0.04
E04	0,066	0,039	0,027	E08	0,059	0,038	0,021
F03	0,075	0,038	0,037	F07	0,07	0,038	0,032
F04	0,082	0,038	0,044	F08	0,085	0,039	0,046
G03	0,079	0,041	0,038	G07	0,067	0,038	0,029
G04	0,078	0,037	0,041	G08	0,071	0,039	0,032
H03	0.114	0,056	0,058	H07	0,055	0,038	0,017
H04	0.08	0,039	0,041	H08	0,062	0,038	0,027

Table A.2: Raw data from HAELISA on secreted adiponectin. Column A is for the control, and B-H has increasing amounts of PLGA particles or standard protein concentration. Each sample was run in duplicate; row 1-2 is the standard curve duplicates and 3-4. 5-6 and 7-8 is the duplicate for day 7, 14 and 19 respectively. MeasA is absorbance with an excitation wavelength of 450 nm, MeasB is measured at 540 nm to determine the well absorbance.